

NAVAL POSTGRADUATE SCHOOL

Monterey, California



THESIS

**AMPLITUDE AND TEMPORAL JITTER ASSOCIATED
WITH THE NPS ACTIVE MODE-LOCKED SIGMA LASER**

by

James A. Anderson

June 2000

Thesis Advisor:
Co-Advisor:

Phillip E. Pace
James H. Luscombe

Approved for public release; distribution is unlimited.

DISC QUALITY INSPECTED 4

20000807 067

REPORT DOCUMENTATION PAGE			<i>Form Approved</i> <i>OMB No. 0704-0188</i>	
Public reporting burden for this collection of information is estimated to average 1 hour per response, including the time for reviewing instruction, searching existing data sources, gathering and maintaining the data needed, and completing and reviewing the collection of information. Send comments regarding this burden estimate or any other aspect of this collection of information, including suggestions for reducing this burden, to Washington headquarters Services, Directorate for Information Operations and Reports, 1215 Jefferson Davis Highway, Suite 1204, Arlington, VA 22202-4302, and to the Office of Management and Budget, Paperwork Reduction Project (0704-0188) Washington DC 20503.				
1. AGENCY USE ONLY (Leave blank)		2. REPORT DATE June 2000	3. REPORT TYPE AND DATES COVERED Master's Thesis	
TITLE AND SUBTITLE : Amplitude and Temporal Jitter Associated with the NPS Active Mode-Locked Sigma Laser			5. FUNDING NUMBERS	
6. AUTHOR(S) Anderson, James A.				
7. PERFORMING ORGANIZATION NAME(S) AND ADDRESS(ES) Naval Postgraduate School Monterey, CA 93943-5000			8. PERFORMING ORGANIZATION REPORT NUMBER	
9. SPONSORING / MONITORING AGENCY NAME(S) AND ADDRESS(ES) N/A			10. SPONSORING / MONITORING AGENCY REPORT NUMBER	
11. SUPPLEMENTARY NOTES The views expressed in this thesis are those of the author and do not reflect the official policy or position of the Department of Defense or the U.S. Government.				
12a. DISTRIBUTION / AVAILABILITY STATEMENT Approved for public release; distribution is unlimited.			12b. DISTRIBUTION CODE	
ABSTRACT (maximum 200 words) Electro-optic techniques for analog-to-digital conversion (ADC) are being developed for wideband signal collection and analysis. They have the capability of being used for direct signal reception and ADC at an antenna. A fundamental requirement for these designs is a high-frequency optical pulse train with uniform amplitude and pulse spacing. A mode-locked fiber laser can provide pulse rates and pulsewidths suitable for these high bandwidth applications. In this thesis an accurate method for calculating and characterizing both the amplitude and timing jitters of the NPS active mode-locked sigma laser was designed and demonstrated. The method utilizes a wide bandwidth photodetector and a microwave spectrum analyzer to obtain data for analysis. Labview 4.0 software was used to extract and store the data displayed on the spectrum analyzer. Matlab 5.1 software was then used to analyze the Labview data and to perform calculations for the amplitude and temporal jitter. Measurements were made for a microwave sweep oscillator and a cw generator, then again with the fiber laser operating with each signal source. Final measurements were taken with variable laser diode pump powers by varying the controller currents. Results show that the calculation of the laser jitter is not dependent on the upper limit of the noise power integral calculation above 10 kHz; however, the jitter is highly dependent on the value of the lower frequency limit and decreases dramatically as the lower limit is increased. Laser amplitude jitter was found to decrease by 30% and timing jitter by 0.85 ps when the laser was operated with the cw generator instead of the sweep oscillator. Also, it was found that as pump power was increased, laser timing jitter decreased.				
14. SUBJECT TERMS Mode-Locked Laser, Sigma Laser, Amplitude Jitter, Temporal Jitter			15. NUMBER OF PAGES 108	
			16. PRICE CODE	
17. SECURITY CLASSIFICATION OF REPORT Unclassified	18. SECURITY CLASSIFICATION OF THIS PAGE Unclassified	19. SECURITY CLASSIFICATION OF ABSTRACT Unclassified	20. LIMITATION OF ABSTRACT UL	

THIS PAGE INTENTIONALLY LEFT BLANK

Approved for public release; distribution is unlimited

**AMPLITUDE AND TEMPORAL JITTER ASSOCIATED WITH THE NPS
ACTIVE MODE-LOCKED SIGMA LASER**

James A. Anderson
Lieutenant, United States Navy
B.S., United States Naval Academy, 1993

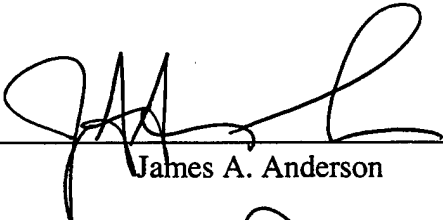
Submitted in partial fulfillment of the
requirements for the degree of

MASTER OF SCIENCE IN APPLIED PHYSICS

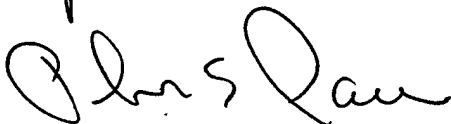
from the

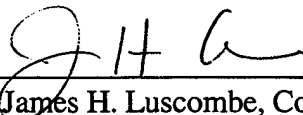
**NAVAL POSTGRADUATE SCHOOL
June 2000**

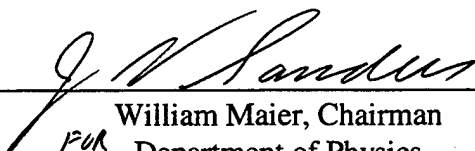
Author:


James A. Anderson

Approved by:


Phillip E. Pace, Thesis Advisor


James H. Luscombe, Co-Advisor


FOR William Maier, Chairman
Department of Physics

THIS PAGE INTENTIONALLY LEFT BLANK

ABSTRACT

Electro-optic techniques for analog-to-digital conversion (ADC) are being developed for wideband signal collection and analysis. They have the capability of being used for direct signal reception and ADC at an antenna. A fundamental requirement for these designs is a high-frequency optical pulse train with uniform amplitude and pulse spacing. A mode-locked fiber laser can provide pulse rates and pulsewidths suitable for these high bandwidth applications. In this thesis an accurate method of calculating and characterizing both the amplitude and timing jitters of the NPS active mode-locked sigma laser was designed and demonstrated. The method utilizes a wide bandwidth photodetector and a microwave spectrum analyzer to obtain data for analysis. Labview 4.0 software was used to extract and store the data displayed on the spectrum analyzer. Matlab 5.1 software was then used to analyze the Labview data and to perform calculations for the amplitude and temporal jitter. Measurements were made for a microwave sweep oscillator and a cw generator, then again with the fiber laser operating with each signal source. Final measurements were taken with variable laser diode pump powers by varying the controller currents. Results show that the calculation of the laser jitter is not dependent on the upper limit of the noise power integral calculation above 10 kHz; however, the jitter is highly dependent on the value of the lower frequency limit and decreases dramatically as the lower limit is increased. Laser amplitude jitter was found to decrease by 30% and timing jitter by 0.85 ps when the laser was operated with the cw generator instead of the sweep oscillator. Also, it was found that as pump power was increased, laser timing jitter decreased.

THIS PAGE INTENTIONALLY LEFT BLANK

TABLE OF CONTENTS

I. INTRODUCTION	1
A. OPTICAL SAMPLING OF WIDEBAND ANTENNA SIGNALS USING MODE-LOCKED LASERS.....	1
B. PRINCIPAL CONTRIBUTIONS	3
C. THESIS OUTLINE.....	5
II. NAVAL POSTGRADUATE SCHOOL ERBIUM FIBER SIGMA LASER	7
A. CAVITY DESCRIPTION.....	7
III. MEASUREMENT AND CHARACTERIZATION OF THE SIGMA LASER ...	11
B. SIGNAL GENERATORS.....	11
1. HP8350B Sweep Oscillator.....	11
2. HP83711B Continuous Wave Generator	12
A. METHOD OF LASER MEASUREMENTS.....	12
1. Photodetector with Spectrum Analyzer.....	14
2. Data Transfer.....	15
B. THEORY OF JITTER MEASUREMENTS	16
1. Amplitude Jitter.....	19
2. Temporal Jitter	20
IV. JITTER MEASUREMENT RESULTS	21

A. PRELIMINARY SPECTRAL ANALYSIS.....	21
B. MICROWAVE SIGNAL GENERATORS.....	25
C. LASER MEASUREMENTS.....	28
1. Amplitude versus Frequency.....	28
2. Laser Jitter.....	31
D. LASER CONTROL AND EFFECTS.....	40
1. Pump Laser Diode Current Setting.....	40
2. Signal Generator Frequency Setting.....	41
VI. CONCLUSIONS AND RECOMMENDATIONS.....	45
A. MEASUREMENT TECHNIQUE.....	45
B. LASER DIODES.....	45
C. DESIGN OF SIGMA LASER.....	46
D. SUMMARY REMARKS.....	46
APPENDIX A. MATLAB CODE FOR SOLVING JITTER CALCULATIONS.....	49
A. AMPLITUDE VERSUS FREQUENCY.....	49
B. AMPLITUDE AND TIMING JITTER.....	51
APPENDIX B. CONFIGURATION AND OPERATION OF THE SIGMA LASER..	55
A. SIGMA LASER OPERATION.....	55
1. Pump Diode Temperature Controller Operation.....	55
2. Pump Diode Laser Controller Operation.....	56

3. Modulation	58
4. Autocorrelator Operation	60
5. Photodetector and Spectrum Analyzer Operation.....	61
6. Autocorrelator Software.....	62
7. Spectrum Analyzer Software	63
8. Turning Off the Sigma Laser	65
 LIST OF REFERENCES	 67
 INITIAL DISTRIBUTION LIST.....	 69

THIS PAGE INTENTIONALLY LEFT BLANK

ACKNOWLEDGEMENT

I would like to thank those who helped me achieve this invaluable goal. First and foremost, I would like to thank Professor Powers, whose constant dedication and vigilance on this project provided me with the direction to success. Another was Professor Pace, whose endless help brought this thesis to completion. Also, Jeff Knight whose assistance with Labview was greatly appreciated.

I would like to dedicate this thesis to my wife Rene, who has stood by me with encouragement, love, and above all an endless amount of patience. She is the center of my life and without her unconditional love and support, I don't think our experience would have been nearly as nice. I look forward to overcoming many more challenges and milestones with her by my side.

Also, to my three lads, Rhett, Cody, and Garrett, you are the lights of my life. Your Daddy loves you and appreciates your support.

This work was supported in part by the Naval Postgraduate School Center for Reconnaissance and the Defense Advanced Research Projects Agency (DARPA).

THIS PAGE INTENTIONALLY LEFT BLANK

I. INTRODUCTION

A. OPTICAL SAMPLING OF WIDEBAND ANTENNA SIGNALS USING MODE-LOCKED LASERS

The use of mode-locked laser pulses to sample wideband microwave signals directly at the antenna is a highly researched area of interest. This direct digitization or digital antenna concept has the capability of turning the analog signal on an antenna into a digital representation without the need for downconversion to intermediate frequencies. The applications for such a capability are evident in communications, electronic warfare, information warfare, and signals intelligence. The bits can be transferred to the receiver signal processing by fiber optics thus eliminating the need for the heavy coax cables that are often used. In the optical analog-to-digital conversion process, the laser pulses are amplitude modulated by the antenna signal using an integrated optical interferometer. The mode-locked laser characteristics that affect the resolution of the resulting digital signal and the bandwidth of the signals that can be digitized are the laser pulse repetition frequency, the pulsewidth, the pulse-to-pulse sample time uncertainty (temporal jitter), and the amplitude uncertainty (amplitude jitter).

Mode-locked lasers produce very short duration pulses in the picosecond range at high pulse repetition frequencies in the gigahertz regime. Optical analog-to-digital converters (ADCs) have sampling frequencies up to 100 times the sampling frequencies of integrated chip ADCs currently available [Ref. 1]. However, optical ADCs that can

digitize a wide bandwidth portion of the RF spectrum (e.g., 10 GHz) with sufficient accuracy (e.g., 10 bits) is a goal that has yet to be achieved.

Calculations have been presented on the maximum pulse width allowable, as well as the maximum amplitude and temporal jitter [Ref. 2]. That is, the sampling waveform will not have pulses of the same amplitude and the space between each pulse will not be uniform. Each pulse will have a small timing error associated with it, otherwise known as timing jitter (σ_J). This jitter will cause the signal sample to be taken at a slightly different time than desired. The maximum timing jitter that can be tolerated without incurring an error greater than one-half a least-significant bit is given by [Ref. 2]

$$\sigma_{J_{\max}} \leq \frac{1}{2^{N+1} \pi f_m} = \frac{1}{2^N \pi f_N}, \quad 1.1$$

where $\sigma_{J_{\max}}$ is the maximum jitter, N is the number of bits in the digitized output, f_m is the highest frequency in the signal, and f_N is the Nyquist sampling rate for the signal ($f_N = 2f_m$). For a 10-bit, 10-GHz bandwidth optical ADC, the Nyquist rate is 20 GS/s and the maximum allowable jitter is 15.5 fs [Ref. 1, 3].

Pulse amplitude jitter is a problem if its variation is significant enough to exceed an ADC step size or least significant bit. A binary-weighted converter with N bits of resolution has $2^N - 1$ quantization levels (approximately $2N$ for most useful values of N). To avoid exceeding a step size, the amplitude variation ΔA must be less than or equal to

$$\Delta A \leq \frac{2A}{2^N} \quad 1.2$$

where $2A$ is the peak-to-peak voltage of the sampled signal. Since amplitude jitter (σ_{AL}), is measured as either a ratio or a percentage of peak value, maximum amplitude jitter can be represented by

$$\sigma_{AL,max} = \frac{100 \Delta A}{A} \leq \frac{100}{2^{N-1}}. \quad 1.3$$

For a 10-bit, 10-GHz bandwidth optical ADC, the maximum tolerable amplitude jitter is to 0.20% [Ref. 1, 4]. By optimizing the design of the mode-locked laser, the possibility of being able to generate high-frequency pulse trains with minimum amounts of jitter can be realized.

One of the more efficient actively mode-locked laser designs is the *sigma laser*. The sigma laser, originally invented at the Naval Research Laboratory (NRL), for high bandwidth optical fiber communications, has an inherently high pulse-repetition-frequency (PRF) due to the unique cavity design that is shaped like the Greek letter sigma (σ). The Naval Postgraduate School (NPS) has adapted this design for use in wideband signal sampling. The characterization of the NPS sigma laser's amplitude jitter and temporal jitter are the subject of this thesis.

B. PRINCIPAL CONTRIBUTIONS

There were five principal goals of this thesis. The first was to develop a user-friendly, accurate method for calculating the amplitude and temporal jitter associated with two separate microwave signal generators. These generators are used to actively mode-lock the laser cavity and determine the pulse repetition interval (PRI). The second goal was to calculate the jitter of the NPS actively mode-locked sigma laser in operation

with each generator. The third was to investigate the dependence of the amplitude and temporal jitter on the limits of integration (f_{high} and f_{low}) of the laser output noise power calculation. The fourth goal was to investigate the effects of the pump diode power on the sigma laser output signal. The two laser diodes are used to pump the optical amplifier. Specifically, how the laser output pulse behaved in the amplitude and frequency domain as the controller current was varied between 32 and 180 mA was also investigated. The final goal was to compare the amplitude jitter effects of the sigma laser at different pulse repetition frequencies.

An accurate method for calculating the jitter associated with the NPS sigma laser was developed using a wide bandwidth photodetector, an RF spectrum analyzer, and a computer. Labview 4.0 computer software was utilized to extract and store the data displayed on the spectrum analyzer using the General Purpose Interface Bus (GPIB) and serial data ports. Matlab 5.1 software was used to perform the jitter calculations on the stored data and produce graphs of the signal amplitude versus frequency. Approximately 40 hours were expended in programming the computer to perform the data calculations.

The data retrieval and calculations were used to study the jitter present in two individual microwave signal generators. By experimentally determining the jitter for both signal generators at a single frequency the best source for actively mode-locking the laser was chosen, resulting in the best stable pulse train. The laser was then operated utilizing both signal generators independently to verify the characterization of the generators.

The amplitude and temporal jitter calculations are functions of the total noise power at the laser output. The noise power was calculated by integrating the power

spectral density with limits of integration ranging from the fundamental PRF (f_{peak}) plus a specified lower frequency limit (f_{low}) to the upper limit of integration (f_{peak}) plus a specified upper limit (f_{high}). Varying the values of f_{high} and f_{low} then graphically presenting the jitter values as each limit was changed extensively tested the dependence of the laser jitter on these limits of integration.

The Naval Postgraduate School sigma laser is unique in that the optical amplifier within the laser is pumped with optical energy using two laser diodes that are current-limited to 181 mA. (Other sigma lasers in operation are usually pumped with much higher power using solid state lasers.) The effects of the laser diode current were tested by varying the current settings on the laser diode controllers and recording the signal of the laser output as a function of amplitude versus frequency.

The final aspect of this research involved comparing the jitter of the laser output signal at different pulse repetition frequencies. Three fundamental frequencies were tested: 5, 7.5, and 10 GHz. The jitter was calculated and compared graphically as a function of the changing limits of integration.

C. THESIS OUTLINE

Chapter II gives an overview of the Naval Postgraduate School (NPS) erbium fiber sigma laser and traces the pulse path through the cavity components. The characteristics of the laser microwave signal generators as well as the method used for jitter measurements are covered in Chapter III. This chapter will also discuss the theory and calculations behind the jitter measurements. Chapter IV presents the results of the

jitter measurements taken. This includes the jitter associated with the signal generators and the laser, the effects of laser diode current settings, and the effects of higher and lower pulse repetition frequency settings. In Chapter V, the thesis conclusions and recommendations are given. They include recommendations for further optimization of the sigma laser as well as possible solutions for jitter reduction. Finally, the Appendices contain the commented Matlab code used to perform the calculations of the jitter and instructions for laser operation.

II. NAVAL POSTGRADUATE SCHOOL ERBIUM FIBER SIGMA LASER

A. CAVITY DESCRIPTION

The Naval Postgraduate School (NPS) sigma laser is similar in design to the patented sigma laser invented at the Naval Research Laboratory (NRL). The NRL sigma laser was originally designed for a 100-GHz, time-domain-multiplexed, fiberoptic communication system [Ref. 5]. Unlike the NRL laser which uses an erbium/ytterbium (Er/Yb) co-doped fiber amplifier pumped by a neodymium (Nd) solid state laser, the NPS sigma laser uses an erbium doped fiber pumped by 200 mW of optical power from two 980-nm pump laser diodes. The NPS sigma laser is unique in that it uses three-fourths less power than the NRL laser but it is powerful enough and stable enough for possible use on small, mobile platforms [Ref 2.].

The NPS sigma laser shown in Figure 2.1 has a light pulse path that travels in a clockwise direction. The path of the light in the cavity is as follows. Two laser diodes pump light at 980 nm through two wavelength division multiplexers into 32 meters of erbium fiber that act as an amplifier. The erbium fiber absorbs the 980 nm light, which raises the energy of the cavity to an upper energy state then releases the energy in the form of 1550 nm light. The light then travels through 80 m of dispersion-shifted fiber to minimize pulse spreading. It then travels through 1 m of dispersion-compensating fiber, shrinking the vertically polarized pulse even more.

Actively Mode Locked Erbium Fiber Sigma Laser - 4/28/98

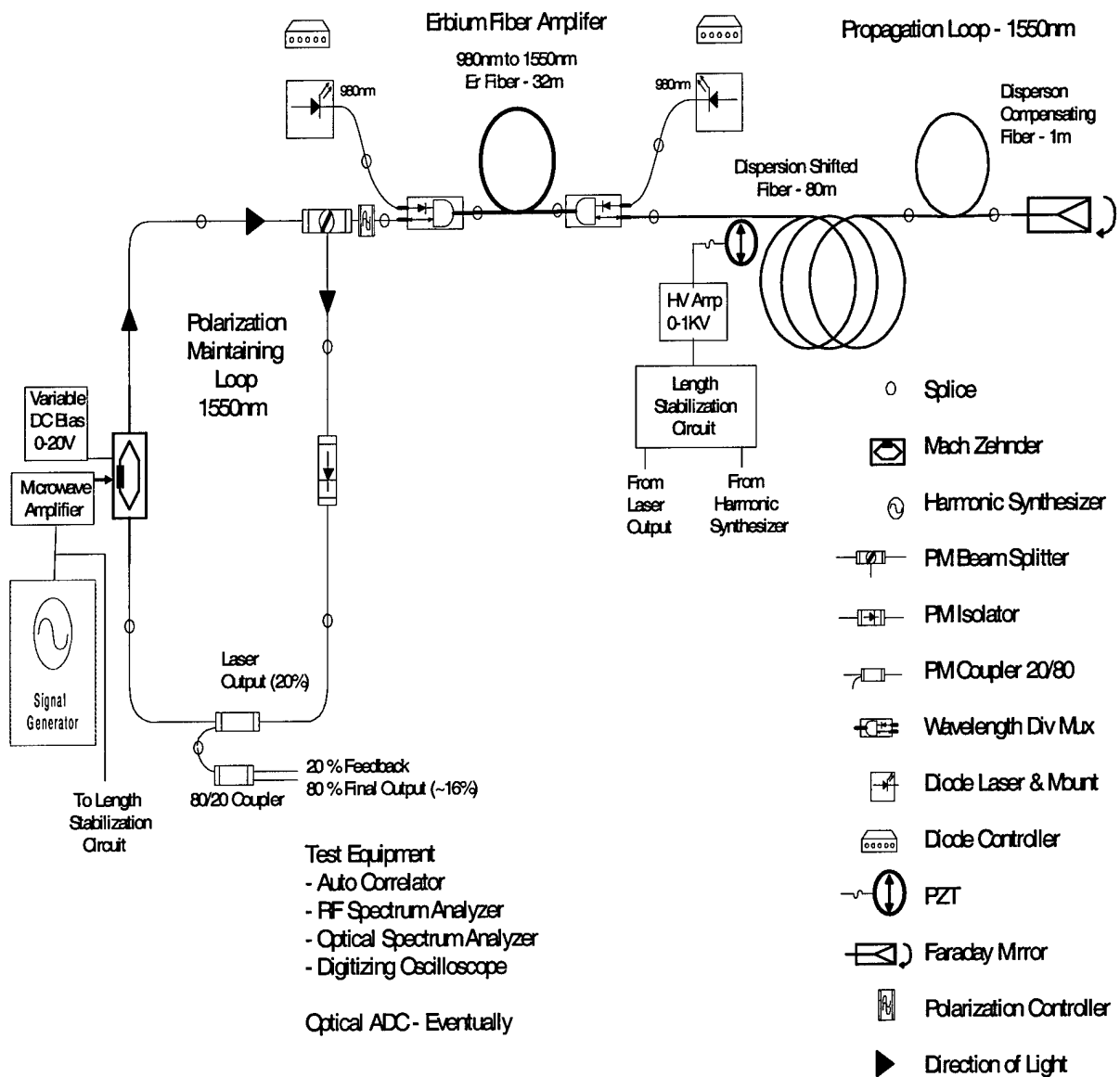


Figure 2.1. Naval Postgraduate School sigma mode-locked fiber laser design.

The light then strikes a Faraday rotating mirror, shifting the vertically polarized light 90° and reflecting horizontally polarized light. The light then travels back through the dispersion-compensating fiber, the dispersion-shifted fiber, and the amplifier, creating an even stronger pulse.

The pulse then enters a polarization controller to ensure a horizontally polarized pulse. The laser pulse then enters the polarization maintaining (PM) loop by passing through a beam splitter that sends the horizontally polarized light down (as indicated by the arrow) through a one-way PM isolator to a PM output coupler. The output coupler splits off a portion of the light, sending 20% of the light to the output. Of the 20% sent to the output, 80% is used as final output and sent to either an autocorrelator or a photodetector and spectrum analyzer. The final output of the laser is approximately 16% of the total light maintained in the laser cavity. The other 20% of the output is sent to a feedback maintaining circuit. The laser light that was not split to the output continues on and enters a Mach Zehnder modulator (MZM).

The MZM modulates the propagation modes within the optical cavity at the PRF determined by the microwave signal generator. Two microwave signal generators were tested, one a sweep oscillator the other a continuous wave generator. Both generators emit sine wave signals at a set fundamental frequency and through the interaction with the laser light in the MZM, the laser pulses "mode-lock" to the desired frequency producing an output signal with a controllable PRF. This is called "active" mode-locking. With an active mode-locked laser, multiple pulses can be maintained within the laser cavity, resulting in a higher pulse frequency. This is opposed to "passive" mode-locking where only one pulse can be maintained within the cavity.

The laser pulse then continues through the PM fiber and hits a special orthogonal splice off-set by 90° causing the orientation of the polarized light to change from horizontal to vertical. The reason for the need to change the polarity of the light, is to enable the light to pass back through the polarizing beam splitter that only allows vertically polarized light to pass. At this point the process repeats.

The one portion of the laser diagram not discussed yet is the length stabilization circuit. The circuit accepts input from the microwave signal generator and 20% of the 20% laser output. Due to thermal differences in the ambient air, the fiber can stretch causing slight differences in the cavity length. The sampled output phase is compared to the signal generator and when they are not the same, a piezoelectric transducer is used to change the cavity length. The change in cavity length cancels the change caused by temperature fluctuations, ensuring a stable PRF.

III. MEASUREMENT AND CHARACTERIZATION OF THE SIGMA LASER

A. SIGNAL GENERATORS

Two microwave signal generators were used to actively mode-lock the NPS sigma laser during the experimental phase of this research. The first generator was the HP8350B Sweep Oscillator and the second was the HP83711B Continuous Wave Generator. The Sweep Oscillator was the earlier piece of test equipment used in the initial laser construction, although no calculations of the jitter for this source alone were performed [Ref 4]. The Continuous Wave Generator was later acquired as an improved signal source. These sources are discussed below in more detail.

1. HP8350B Sweep Oscillator

The Hewlett-Packard model 8350B Sweep Oscillator used during the initial design of the NPS Fiber Laser was modified with a Hewlett-Packard model 83592 RF Plug-in installed. The range of the RF Plug-in unit was 0.01 – 20.0 GHz. The sweep oscillator was run in continuous wave mode with the sweep trigger set to INTERNAL [Ref 4]. Through experimentation, it was found that this signal generator was power limited at higher frequencies, resulting in an “unleveled” indication on the generator. Thus, the “power level” had to be reduced when fundamental frequencies above 10.0 GHz were used. This was accomplished by decreasing the “power level” in 0.1 dBm increments until the “unleveled” fault ceased. Secondly, the signal produced by this generator tended to drift slightly during laser operation resulting in the use of the feedback-compensating loop more often.

2. HP83711B Continuous Wave Generator

The Hewlett-Packard model 83711B Continuous Wave (cw) Generator was purchased to replace the sweep oscillator. It provided a stable cw source in the range of 1.0 – 20.0 GHz. The cw generator was also power limited at higher frequencies, but the “power level” only required adjustment for signals greater than 14.0 GHz. This device also utilized an INTERNAL trigger to produce the output signal. The initial benefit of this device was that during laser operation, there seemed to be no appreciable signal drift, allowing for a stable sampling source.

B. METHOD OF LASER MEASUREMENTS

In its current form, the NPS sigma laser is capable of providing a range of pulse rates from 2 to 12 GHz. There are a number of measurement techniques available that provide accurate data analysis of the laser signal. The research in this thesis was based on the theory of laser noise measurements. The measurements were accomplished by channeling the final pulsed output of the laser signal through a fast photodetector. An RF spectrum analyzer was coupled to the output of the photodetector for measurement. The data displayed on the spectrum analyzer was then transferred to a computer via a GPIB interface for storage and analysis. The final output of the laser signal is approximately 16% of the total laser light resonating in the cavity [Ref. 4]. This amount was suitable for measurement purposes. Table 4.1 lists all measurement equipment used and the connector types.

Device Nomenclature	Connector
ILX Optical Multimeter (OMM-6810) with OMH-6706 Measurement Head	FC/ST
Femtochrome FR-103MN/IR Autocorrelator	FC
Hewlett Packard 8566B RF Spectrum Analyzer	
Newport/Picometrix D-15ir Photo-Detector with attached DC Block	ST
Hewlett Packard 8350B Sweep Oscillator	
Hewlett Packard 83711B Continuous Wave Generator	

Table 3.1. List of Test and Measurement Equipment.

Figure 3.1 shows the general layout of the measurement equipment and connections. The photodetector, in conjunction with the RF spectrum analyzer, was used to take all measurements. By attaching an ST/FC patch cord to the output pigtail of the sigma laser, the autocorrelator with the oscilloscope could also be used for pulsewidth measurements. However, the autocorrelator was being repaired so no pulsewidth measurements were made for this thesis.

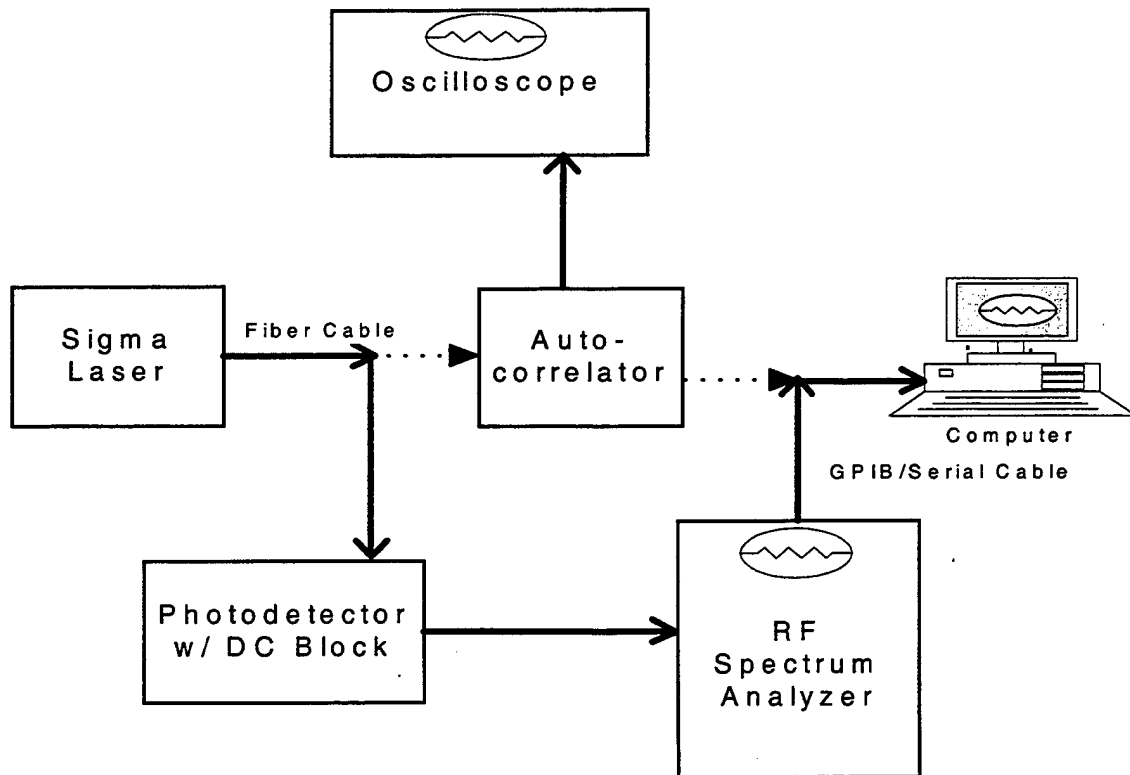


Figure 3.1. Test and measurement equipment layout with connections.

1. Photodetector with Spectrum Analyzer

The laser measurements were accomplished with the use of a Newport D-15ir fast photodetector in conjunction with a Hewlett-Packard 8566B RF spectrum analyzer. The sigma laser was mode-locked at pulse repetition frequencies of 2 to 12 GHz. The photodetector had a 26 GHz detection bandwidth and a conversion factor of 23.46 mV per mW of light energy [Ref. 6]. A dc block was used at the output of the photodetector to protect the spectrum analyzer from low dc voltage present in the photodetector. The dc Block had a measured insertion loss of 1 dB [Ref. 4].

The HP8566B spectrum analyzer has a frequency range of 2 to 22 GHz with a sweep time (ΔT) of 60 ms and can store up to 1000 data points of information. Figure 3.1 shows that the spectrum analyzer was connected to a computer using a GPIB/Serial cable. Labview 4.0 software was used to create a program to extract stored data from the spectrum analyzer memory, to display it on the computer screen, and then to store this data on the computer hard drive as a "text" file for later analysis. One characteristic of this particular spectrum analyzer was that the spacing on the frequency axis was dependent on the frequency span that was manually programmed on the analyzer itself. The frequency span was automatically broken into 1000 equally spaced bins and the points recorded. In other words, a signal being generated on the spectrum analyzer with a frequency span of 2 MHz had data points recorded every 2000 Hz. Since all of the measurements, discussed later in this chapter, required data of a 2 MHz span and as close to the peak frequency as possible, two separate files of information were required. The first file contained data for a span of 2 MHz and the second file contained data for a frequency span of 20 kHz. With these two files there were a total of 2000 points of data

for a single signal. They are combined to provide data ranging from the peak signal frequency plus 20 Hz out to the peak signal frequency plus 1 MHz for an input PRF of 2 GHz.

2. Data Transfer

The signal image generated on the spectrum analyzer was transferred to the computer and displayed by a virtual instrument (vi) program written using Labview 4.0 software. It should be noted that the image seen on the Labview screen was not a screen dump or bit map of the spectrum analyzer screen, but rather the image created by the array of 1000 data points embedded in the spectrum analyzer memory. Figure 3.2 shows an example of the Labview image for a 10-GHz PRF laser signal from the spectrum analyzer. The image that Labview produced using the spectrum analyzer data points was similar to the spectrum analyzer image and had frequency in units of Hz plotted on the x-axis and amplitude in units of dBm plotted on the y-axis. The data points, extracted and recorded by Labview, to the 12th significant digit, were then saved as a 2-column, 1000-row array text file for later analysis using programs written in Matlab version 5.1.

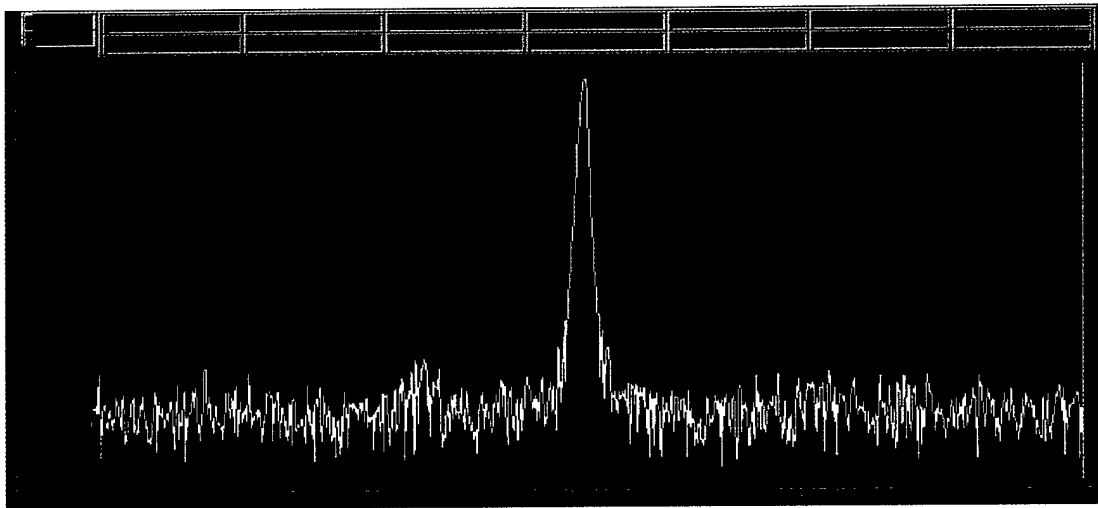


Figure 3.2. Labview 4.0 virtual instrument display of 10 GHz laser signal. 1000 data points at a frequency span of 2 MHz.

C. THEORY OF JITTER MEASUREMENTS

The shape of the pulses from the NPS sigma laser consist typically of a short pulse superimposed upon a much longer lower-amplitude pulse commonly referred to as a “pedestal.” The pedestal results in an undesired variation in the frequency response in sampling measurements at frequencies on the order of the inverse of the pedestal time duration. A signal produced from a mode-locked laser has many different types of noise associated with it. The two that have the most prevalent effect on the optical sampling of microwave signals, and thus the subject of this thesis research, are amplitude jitter and temporal jitter. Amplitude jitter refers to the small amplitude fluctuations occurring in the detection bandwidth while timing jitter (or phase noise) produces fluctuations in the pulse repetition interval of the laser.

The measurement of the laser jitter was difficult in the time domain. Since we were unable to measure the pulse (no autocorrelator available), it was not possible to

resolve its position to the femtosecond accuracy that was required. Also, autocorrelation usually gives inadequate information about amplitude noise due to the limited receiver bandwidth. In addition, no information on the higher-frequency background intensity noise and timing jitter of the laser can be gained [Ref. 7]. Consequently, jitter measurements were accomplished by computations based on power spectrum techniques in the frequency domain using the RF spectrum analyzer. Figure 3.1 shows the noise spectrum at the base of a mode-locked laser signal.

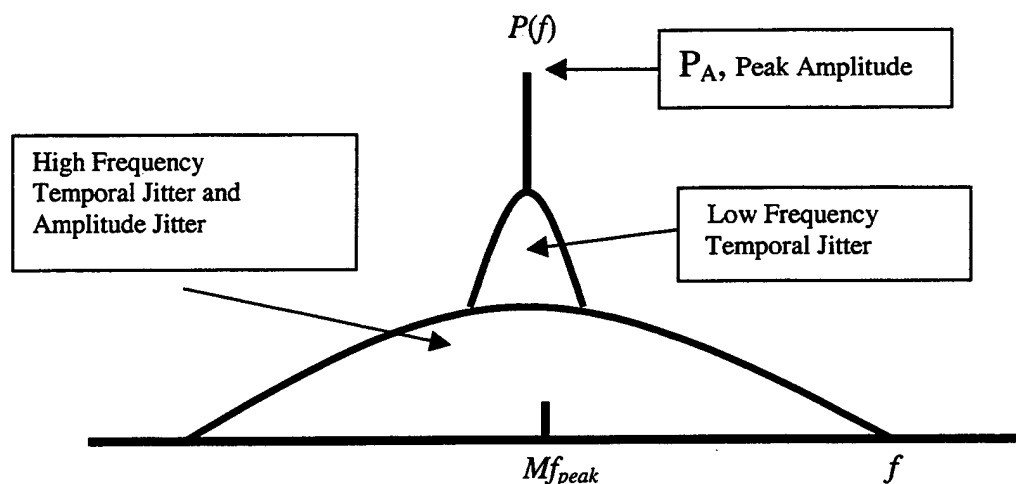


Figure 3.2. Noise spectrum for a mode-locked laser signal in the frequency domain [Ref. 7].

The measured fundamental PRF is f_{peak} and the harmonic number is M . For the case of the fundamental, $M = 1$. The peak amplitude is P_A . The amplitude-noise sidebands dominate at lower laser harmonics, while the phase-noise sidebands, having power proportional to M^2 , dominate for harmonics of higher order. Thus, the amplitude noise is determined by measuring the sidebands on a low laser harmonic while timing jitter (phase noise) is determined by measurements on a sufficiently high harmonic. For the timing jitter measurement, it should be verified that the chosen high-harmonic-noise

sidebands are not dominated by amplitude noise, however, this was not possible due to the frequency limitations of our spectrum analyzer.

Spectrum analyzers display the power spectral density $P(f)$ integrated over the analyzer resolution bandwidth (rbw) as a function of the frequency f . The noise power P_N , used to compute the amplitude and timing jitter, is calculated by integration of the power density [Ref. 8]

$$P_N(M, f_{high}, f_{low}) = (2/rbw) \int_{Mf_{peak} + f_{low}}^{Mf_{peak} + f_{high}} P(f) df \quad 3.1$$

and is a function of the harmonic number M and the frequency span $[f_{high}, f_{low}]$.

The sweep time or measurement duration ($\Delta T = 60 \text{ ms}$) determines f_{low} by the relationship $f_{low} = 1/4\Delta T = 4.16 \text{ Hz}$. Amplitude fluctuations and timing jitter components with frequencies below this value contribute little to changes in the laser intensity and timing observed over the period ΔT [Ref. 8]. The detection bandwidth of the measurement determines f_{high} .

The spectrum analyzer provided 1000 points of data covering the frequency *span* selected. The frequency separation Δf between these data points was the frequency span divided by 1000 ($span/1000$). Integration was accomplished by using a finite sum to approximate the integral [Ref. 9]. Replacing the integral with the finite sum, the integration of the power density becomes

$$P_N(M, f_{high}, f_{low}) = (2 / rbw) \sum_{n=1}^{500} P_{mw}(n\Delta f) \quad 3.2$$

where,

$$P_{mw}(n\Delta f) = 10^{\frac{P(n\Delta f)}{10}} \quad 3.3$$

converting to linear units and n represents the index into the spectrum data in the span $(Mf_{peak} + f_{low}, Mf_{peak} + f_{high})$. One aspect of this thesis research was to explore the dependence of the laser jitter calculations on the limits of integration.

1. Amplitude Jitter

Amplitude jitter (σ_{AL}) is the slight variation in the amplitude or height of a pulse. It is expressed as either a ratio of noise power to peak amplitude power or as a percentage. Amplitude jitter dominates over temporal jitter when measured at the fundamental frequency. The calculation of the rms amplitude jitter for a given frequency span is given by [Ref. 8]

$$\sigma_{AL} [Mf_{peak} + f_{low}, Mf_{peak} + f_{high}] = \sqrt{P_N / P_A} \quad 3.4$$

where P_A is the peak power of the carrier. As the equation stands, this will give a unitless result, but multiplication of this value by 100 will give the amplitude jitter as a percentage. All of the amplitude jitter diagrams contained in this thesis are graphed using σ_{AL} in its unitless form. Numerical comparisons are made as noise power as a percentage of fundamental frequency peak power.

2. Temporal Jitter

Timing jitter is a function of the PRI or period of the laser pulse and subsequently is measured in seconds. The temporal jitter or timing jitter (σ_J) represents fluctuations of the PRI ($1/f_{peak}$). Temporal jitter has a power proportional to the square of the harmonic (M^2). When present in the higher harmonics, it will dominate over amplitude jitter.

Timing jitter in sampling experiments degrades the time resolution and gives rise to additional noise in the measurement [Refs. 7, 8]. The calculation for the temporal jitter (σ_J) is [Ref. 8]

$$\sigma_J = \left(\frac{PRI}{2\pi M} \right) \sigma_{AL} = \left(\frac{1}{2\pi M f_{peak}} \right) \sqrt{\frac{P_N}{P_A}} \quad 3.5$$

The temporal jitter is measured at higher harmonics. However, due to the 20-GHz upper frequency limit of the spectrum analyzer, the desire to characterize harmonics of a 10-GHz signal could not be accomplished. The measurements for the jitter were subsequently taken with a PRF of 2 GHz, with the amplitude jitter calculated at the fundamental, and the timing jitter calculated at the 5th harmonic or a PRF of 10 GHz.

IV. JITTER MEASUREMENT RESULTS

A. PRELIMINARY SPECTRAL ANALYSIS

During the course of research, the first step was to construct a simple, accurate, and user-friendly process for analyzing and measuring the jitter of a signal from the sigma laser. As discussed earlier, 1000 data points, representing the laser signal were stored as text files using Labview 4.0 software. These text files were used in two computer programs written in Matlab 5.1 code, that allowed the user to import 8 separate data text files, two files of data per signal sampled. The programs provided the ability to compare the amplitudes versus frequency graphically, to compute the amplitude and high frequency temporal jitter for each file, and then to compare these results. One limitation that was encountered was the ability to compute the jitter measurements as close to the peak frequency as possible. The reasons for this were two fold. The first was due to the limitation of the spectrum analyzer to resolve discrete data points at large frequency spans. The second was due to the degeneration of the laser signal below a 20-kHz frequency span. This posed a problem in that the spectrum analyzer measurement duration ($\Delta T = 60$ ms) required a power spectrum density integration from the peak frequency plus 4 Hz out to a range of 1 MHz. To solve this problem, a process was established where a signal was sampled with a frequency span of 2 MHz and recorded. Then that same signal was sampled again at a frequency span of 20 kHz and recorded. The Matlab computer programs were then written so that two integrals (replacing with

finite sums) were added together in the P_N calculations. The resulting equation for P_N was

$$P_N = (2 / rbw) \left[\underbrace{\sum_{n=1}^{500} P_{mW}(n \Delta f)}_{20 \text{ kHz span}} + \underbrace{\sum_{n=1}^{n=500} P_{mW}(n \Delta f)}_{2 \text{ MHz span}} \right] \quad 4.1$$

The first summation covers the portion of the spectrum from f_{low} to $(f_{low} + 10)$ kHz; The second summation covers the spectrum from $(f_{low} + 10)$ kHz to $(f_{low} + 1)$ MHz. This allowed for the analysis of a fundamental signal for the full range with the lower limit as close to 4 Hz as the spectrum analyzer could resolve. In the case of the 2 GHz signal, the lower limit was 20 Hz.

The signals produced by the microwave generators were set at a frequency of 2-GHz. The spectrum analyzer was able to detect the 10-GHz 5th harmonic of the 2-GHz signal hence, the timing jitter was calculated from the 5th harmonic of the 2 GHz fundamental PRF. Using the first harmonic of the 2 GHz signal provided accurate amplitude jitter comparisons. One aspect of this research involved the behavior of the laser jitter as a function of the limits of integration. Consequently, all of the graphical analysis contained in this thesis involving amplitude or timing jitter at the fundamental frequency were displayed as a function of the change in f_{high} or the change in the lower frequency limit f_{low} .

It was predicted that by varying f_{high} , the amplitude and timing jitter would remain relatively constant at some point. The data was collected and plotted. Figure 4.1 and 4.2, respectively, show the amplitude and temporal jitter results for the HP83711B CW Generator as the upper limit f_{high} was changed from 2 kHz to 1 MHz .

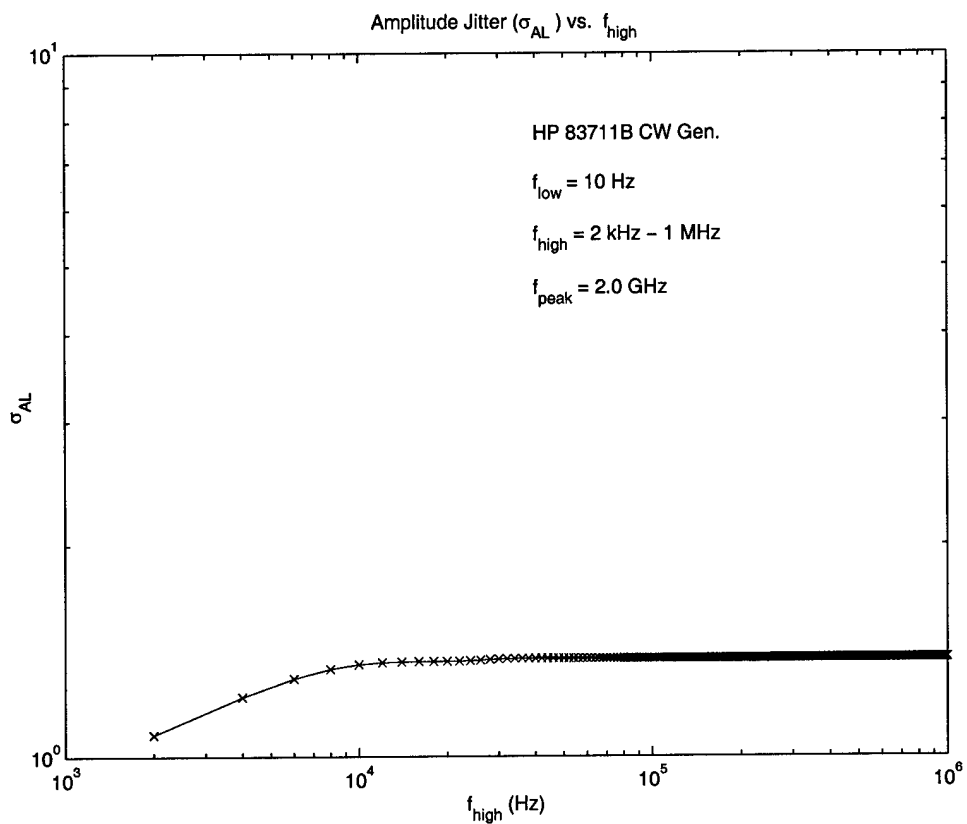


Figure 4.1. Amplitude jitter for the HP83711B CW generator as a function of the upper limit of integration.

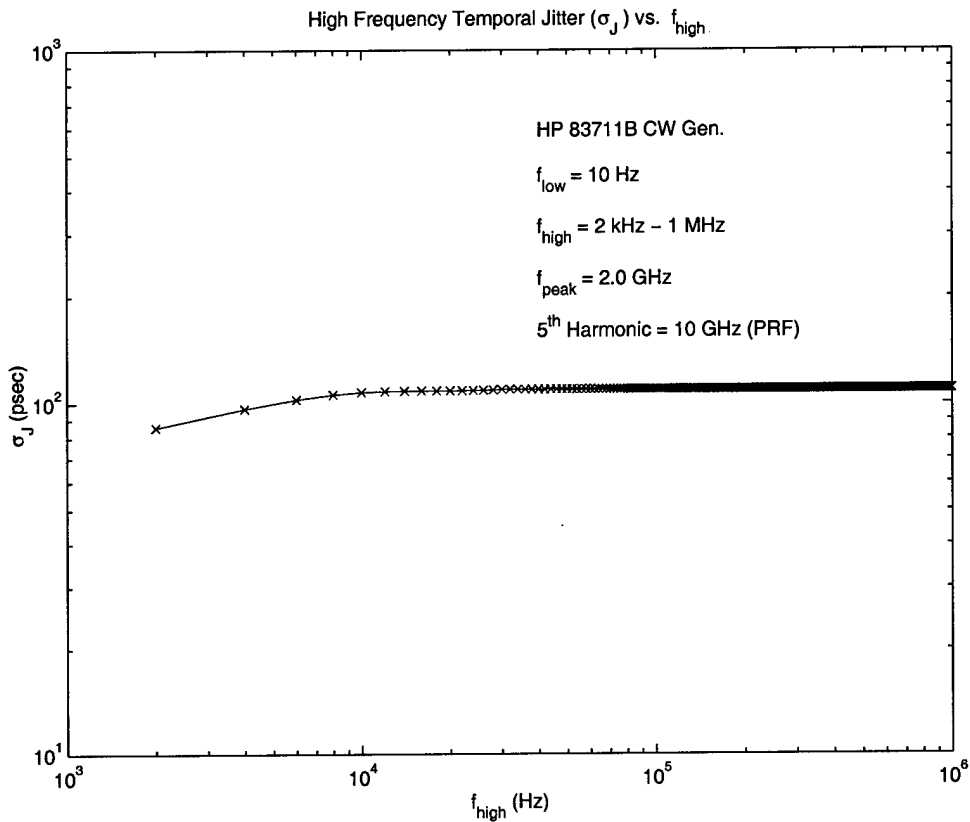


Figure 4.2. Timing jitter for the HP83711B CW generator as a function of the upper limit of integration.

Based on the above two plots, it can be noted that changing the upper limit of integration f_{high} past 10 kHz, had no appreciable affect on the jitter measurements. Because of this, the upper limit of integration was kept constant at a convenient 1 MHz, vice the detector bandwidth of 26 GHz, and the focus placed on the effect of changing the lower limit of integration, f_{low} . Subsequent graphs and diagrams were plotted as a function of the change in the lower limit of integration (f_{low}).

B. MICROWAVE SIGNAL GENERATORS

The next step was quantifying the jitter produced by the HP8350B Sweep Oscillator and the HP83711B CW Generator. To accomplish this, both generators were disconnected from the laser and attached directly to the spectrum analyzer. A nominal frequency of 2 GHz was used as the test frequency. Measurement data was taken for both generators for frequency spans of 20 kHz and 2 MHz. This data was first plotted in the frequency/amplitude domain to identify fundamental differences in the signal spectrums. Figure 4.3 shows the signal fundamental produced by the generators as referenced to 0 dBc (dB relative to the amplitude of the fundamental PRF). The signals begin at peak frequency plus 2 kHz out to 700 kHz.

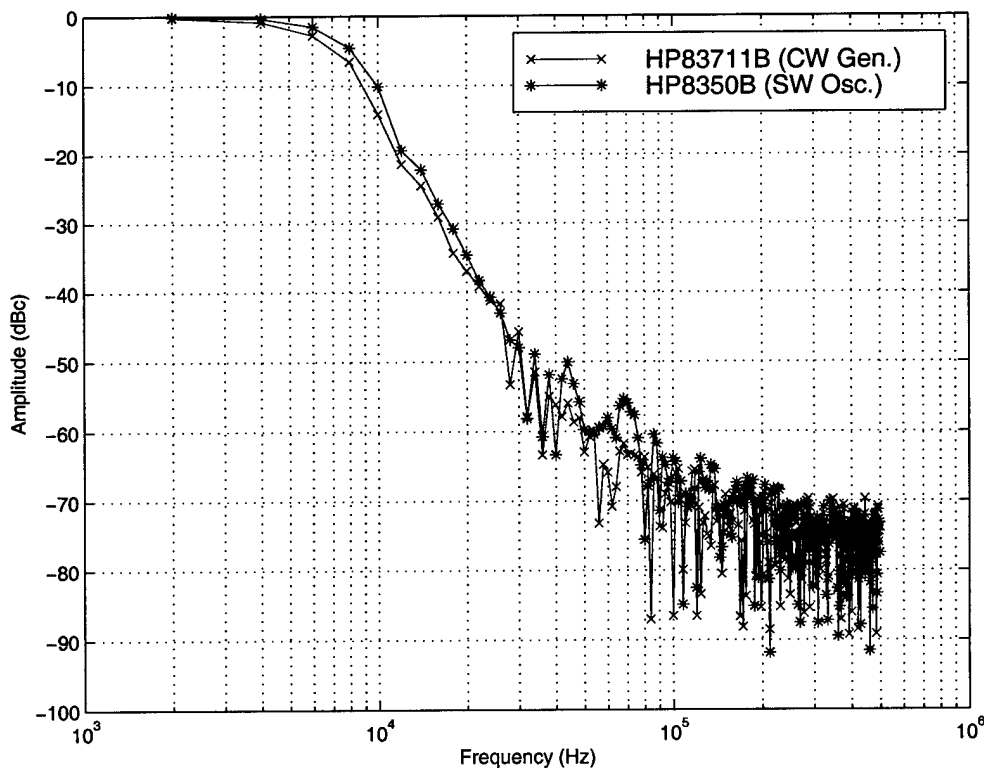


Figure 4.3. CW generator and sweep oscillator frequency and amplitude comparison.

As shown in Figure 4.3, the amplitude characteristics from the two generators differ only slightly. The inherent noise in the sweep oscillator, however, was slightly more pronounced.

The next step in comparing these two signal generators was to perform the jitter calculations at the fundamental with a changing lower limit of integration to quantify what effect the reduced bandwidth had on the total jitter. The integration was performed by changing f_{low} from 20 Hz to 5 kHz, with f_{high} held constant at 1 MHz.

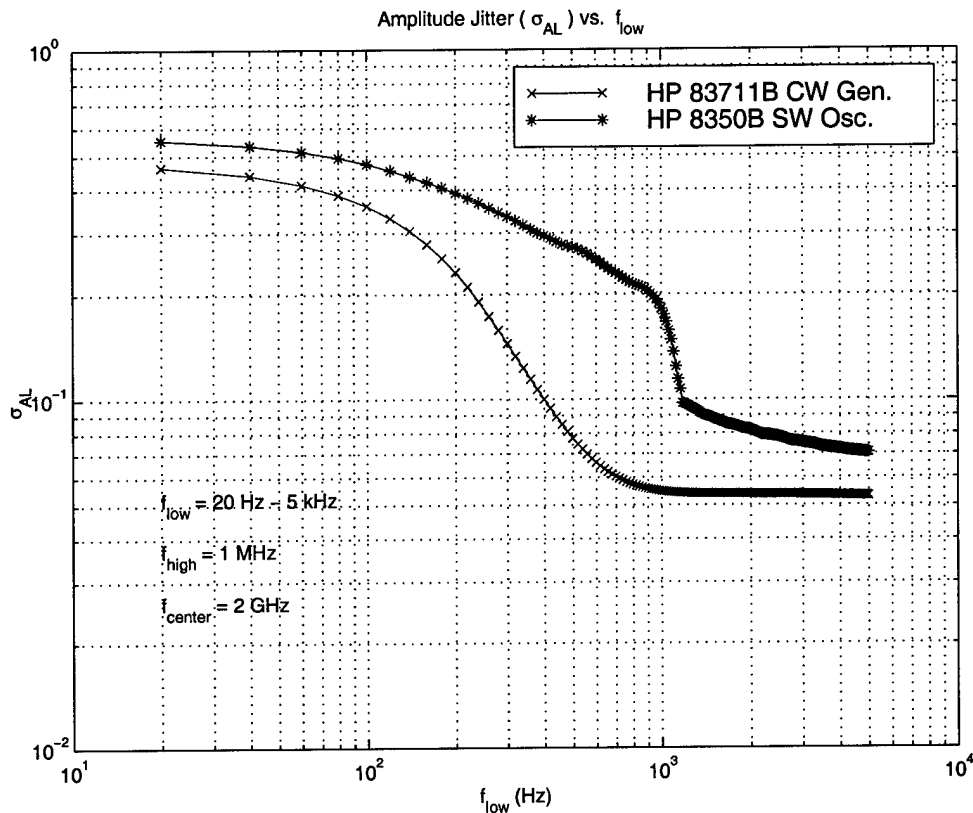


Figure 4.4. CW generator and sweep oscillator amplitude jitter comparison.

Figure 4.4 shows a comparison of the amplitude jitter between the sweep oscillator and the cw generator. The numerical value of the maximum amplitude jitter for

each generator was calculated by reading the graphical value of the amplitude jitter ratio for $f_{low} = 20$ Hz and multiplying by 100 to obtain the percentage. For the cw generator, the maximum amplitude was measured at approximately 46% of the fundamental peak amplitude, while the sweep oscillator was 56%.

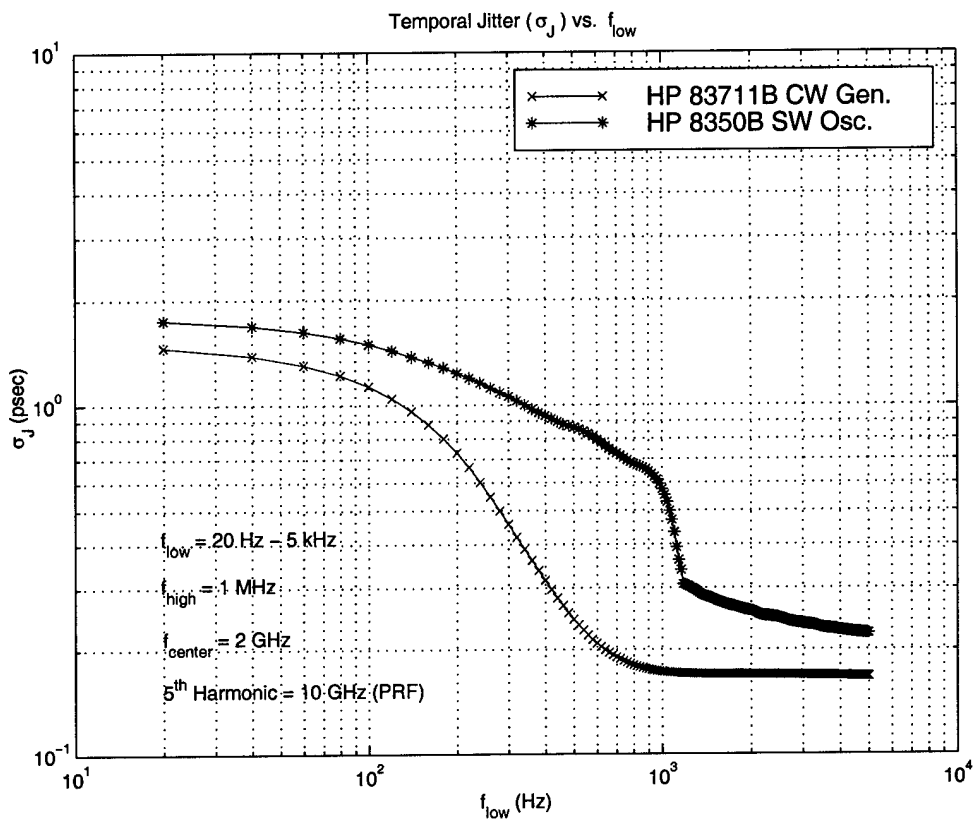


Figure 4.5. CW generator and sweep oscillator temporal jitter comparison.

Figure 4.5 shows the temporal jitter comparison for the two generators. A difference of 0.35 ps of timing jitter at the maximum frequency span can be seen between the cw generator and the sweep oscillator. Both the timing jitter and amplitude jitter graph show that the cw generator's signal is more likely to provide a more stable pulse

train in the overall performance of the sigma laser. Quantifying the jitter of both generators allows for the selection of the source that will provide the best laser output.

C. LASER MEASUREMENTS

1. Amplitude versus Frequency

While it was required to analyze the sigma laser jitter to promote future design initiatives, knowing how individual devices within the laser behave gave a better understanding of the entire jitter measurement process. With the individual signal generators characterized as to amplitude and timing jitter, they were re-introduced to the sigma laser circuit loop and measurements taken. The first step was to analyze the amplitude versus frequency for each source individually and compare that to the amplitude versus frequency for that source in conjunction with the sigma laser.

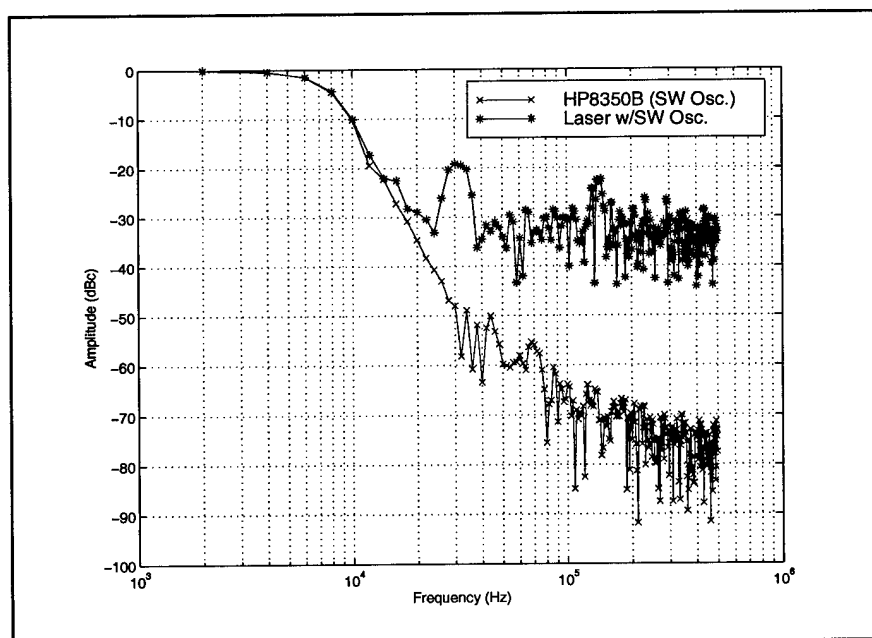


Figure 4.6. Laser and sweep oscillator, frequency and zeroed amplitude comparison.

Figure 4.6 shows the comparison of the sweep oscillator signal and the sigma laser operating with the sweep oscillator. In both cases, the sweep oscillator was transmitting a 10 GHz pulse with a frequency span between 2 kHz and 500 kHz. Both of the signals were referenced to zero dBc. The amplitude of the laser signal was significantly reduced with respect to the pure sweep oscillator signal. A sidelobe at 30 kHz was also present in the laser output. Some reduction in amplitude was expected. The effect on the overall jitter of the system will be discussed later.

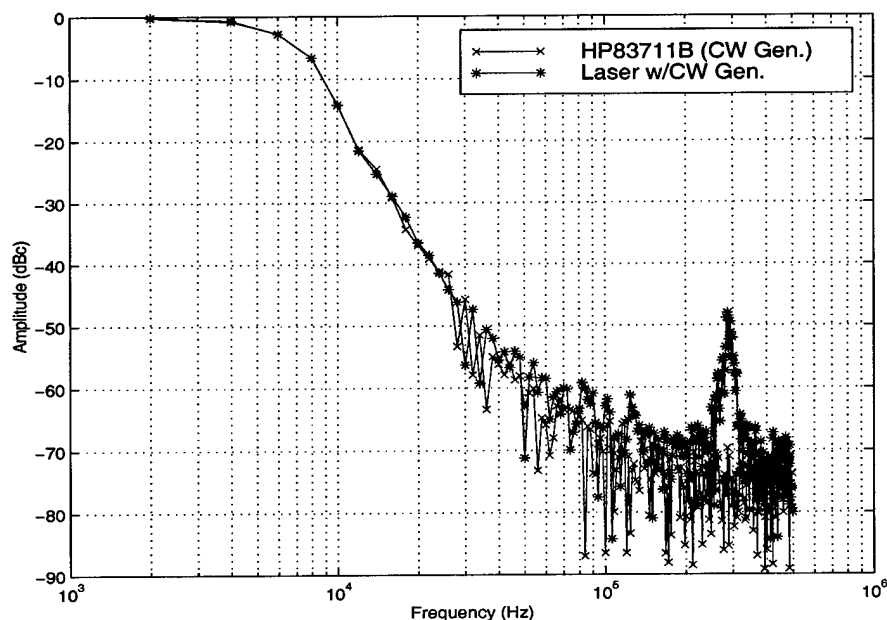


Figure 4.7. Laser and CW generator, frequency and zeroed amplitude comparison.

Figure 4.7, like Figure 4.6, was a comparison of the signal produced from the cw generator and the signal of the sigma laser operating with the cw generator installed. These measurements were made with a 10-GHz signal and a frequency span between 2

kHz and 500 kHz. A sidelobe at 300 kHz was present in the laser output. Overall, the continuous wave generator seemed to produce a narrower laser spectrum line width as compared with the sweep oscillator. This is further clarified in Figure 4.8, which shows a comparison of the two laser signals in the frequency and amplitude domain.

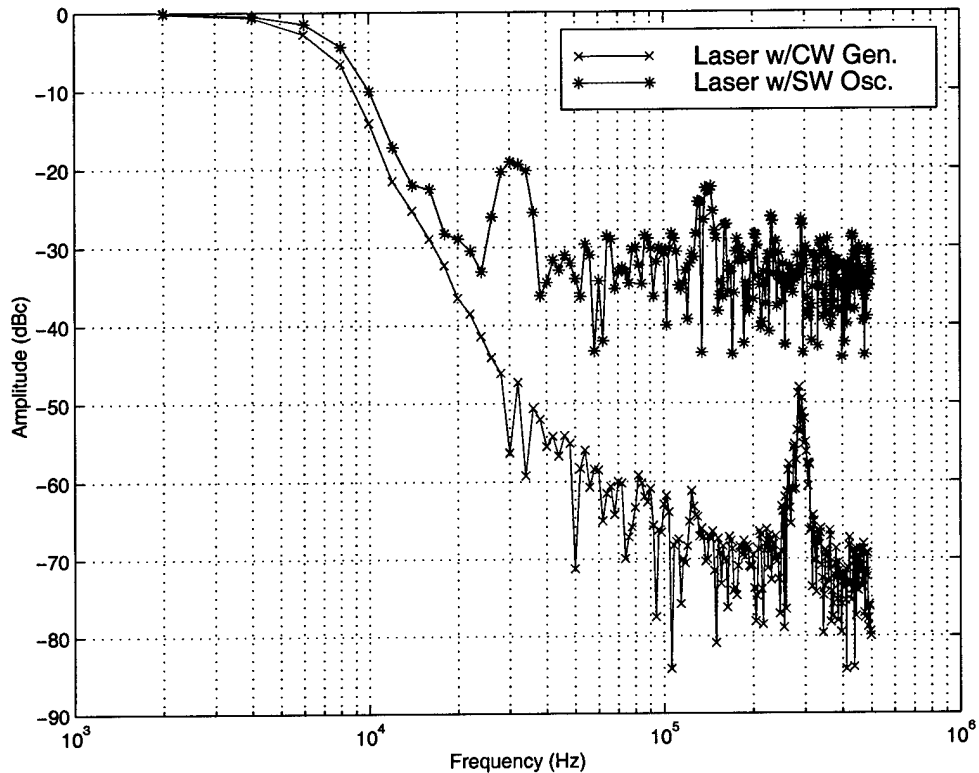


Figure 4.8. Laser powered by CW generator and sweep oscillator, frequency and zeroed amplitude comparison.

With the spectra of the sigma laser and the signal sources graphically analyzed and the jitter measurements complete for the individual signal sources, the generators were re-applied to the laser and jitter calculations completed.

2. Laser Jitter

Based on the amplitude versus frequency plots discussed earlier, it was predicted that the amplitude and temporal jitter associated with the laser would be greatest when the sigma laser was used in conjunction with the sweep oscillator. How much of a difference was unknown. The jitter measurements for the laser were accomplished in the same manner as the measurements for the signal generators. A laser pulse frequency of 2 GHz was used as the nominal frequency for all tests. A lower limit of integration range, f_{low} , of 20 Hz to 5 kHz was used, with f_{high} held constant at 1 MHz.

The first test was conducted using the sigma laser with the sweep oscillator.

Figure 4.9 shows the graphical results of the amplitude jitter versus f_{low} for the sigma laser and the sweep oscillator signal.

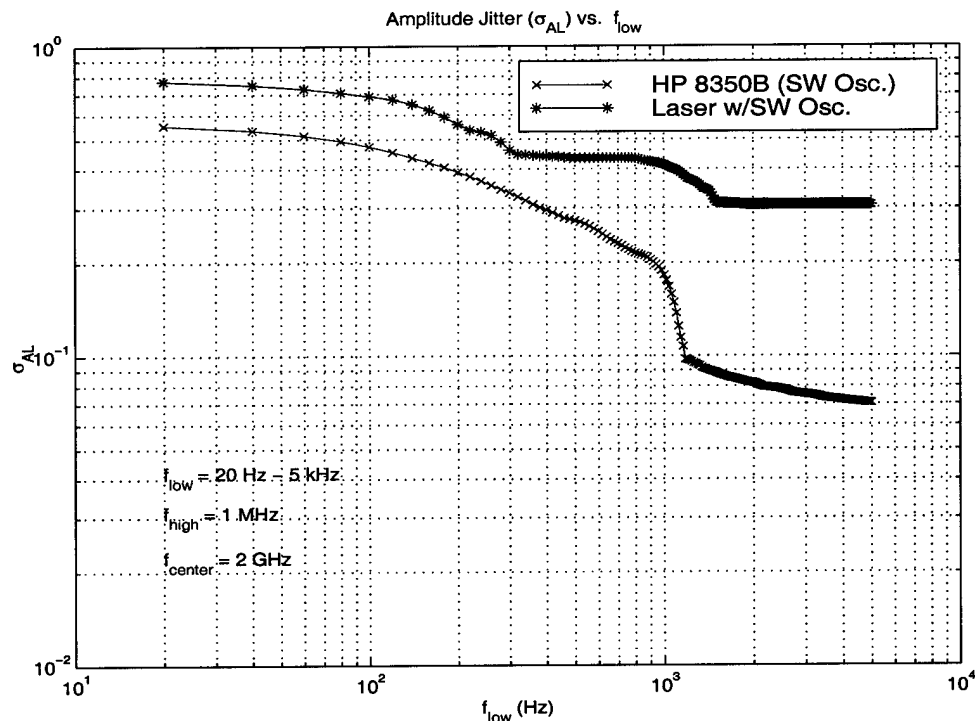


Figure 4.9. Sweep oscillator and Laser powered by sweep oscillator, amplitude jitter comparison.

By taking the data for the maximum frequency span for the amplitude jitter displayed in Figure 4.9 and multiplying by 100, the amplitude jitter as a percentage of peak amplitude was derived. Figure 4.9 shows that the amplitude jitter, with f_{low} equal to 20 Hz, for the sigma laser when used with the sweep oscillator was nearly 78% of the peak signal.

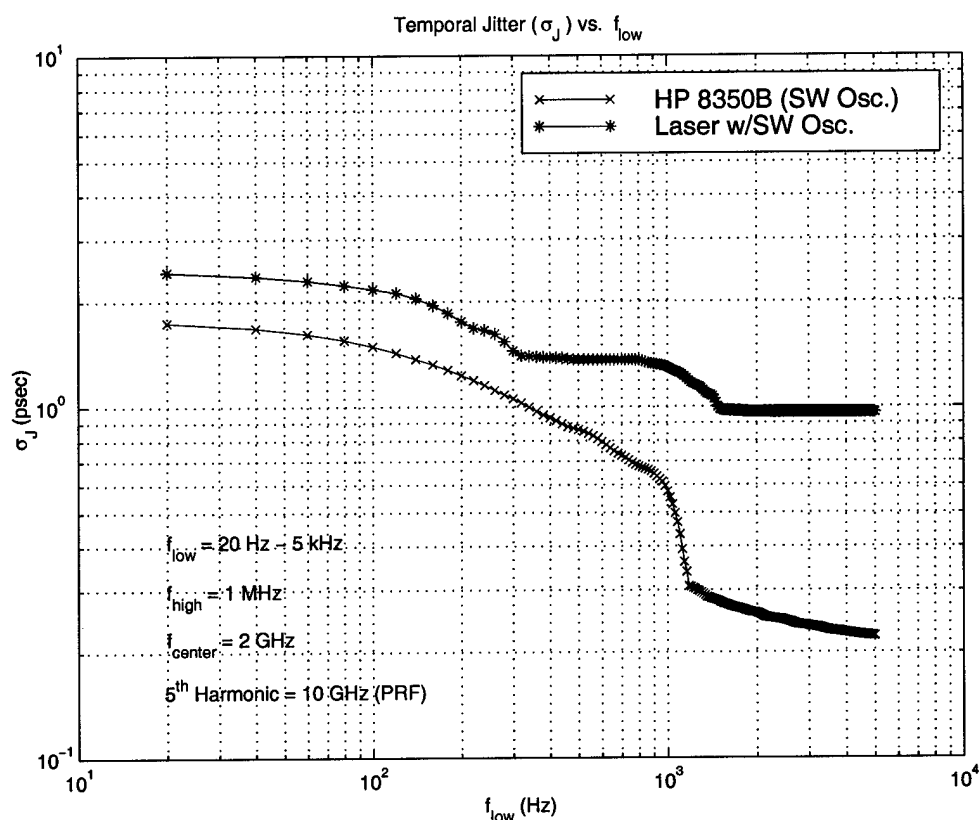


Figure 4.10. Sweep oscillator and laser powered by sweep oscillator, timing jitter comparison.

Figure 4.10 shows the temporal jitter comparison for the sigma laser and the sweep oscillator measured at the 5th harmonic. The timing jitter, σ_J , was measured in picoseconds (ps). The graph shows the sweep oscillator with approximately 1.8 ps of

timing jitter, while the sigma laser shows 2.5 ps of fluctuation between pulses when f_{low} was 20 Hz.

The next test was performed on the laser and the continuous wave generator. All of the test parameters were held exactly the same as with the laser and the sweep oscillator.

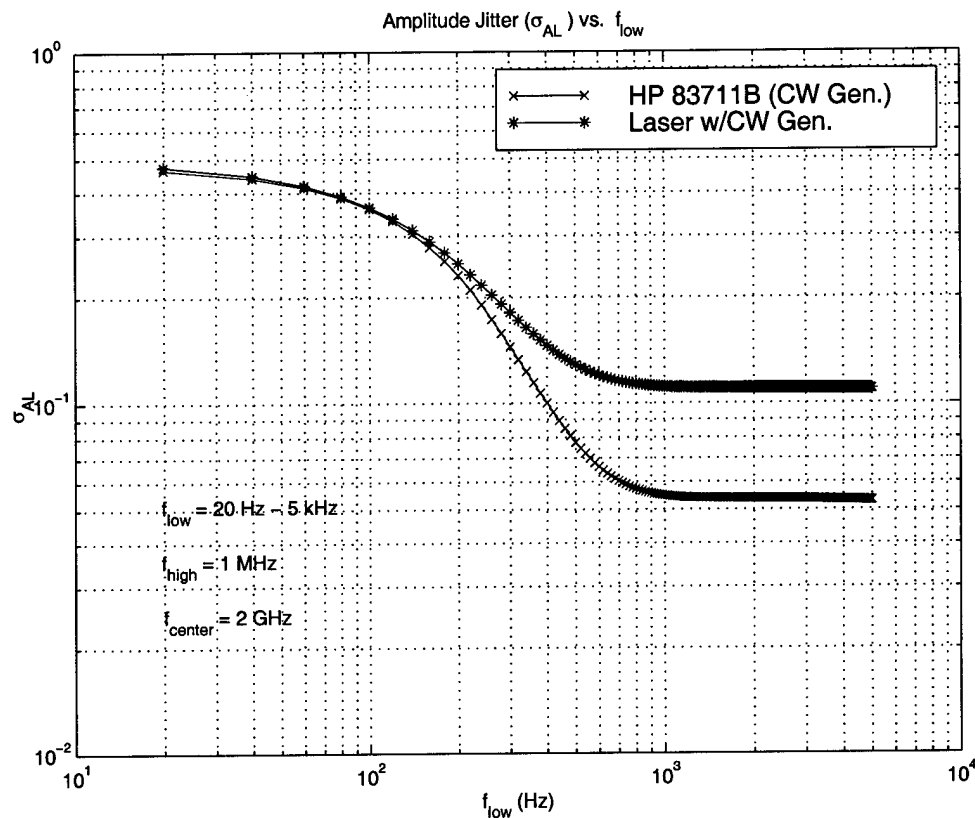


Figure 4.11. CW generator and laser powered by CW generator, amplitude jitter comparison.

Figure 4.11 shows that the amplitude jitter of the continuous wave generator was approximately 46% of the peak frequency. The figure also shows that the laser with the cw generator had an amplitude jitter of nearly the same amount.

The next step was to compare the timing jitter for the cw generator and the laser.

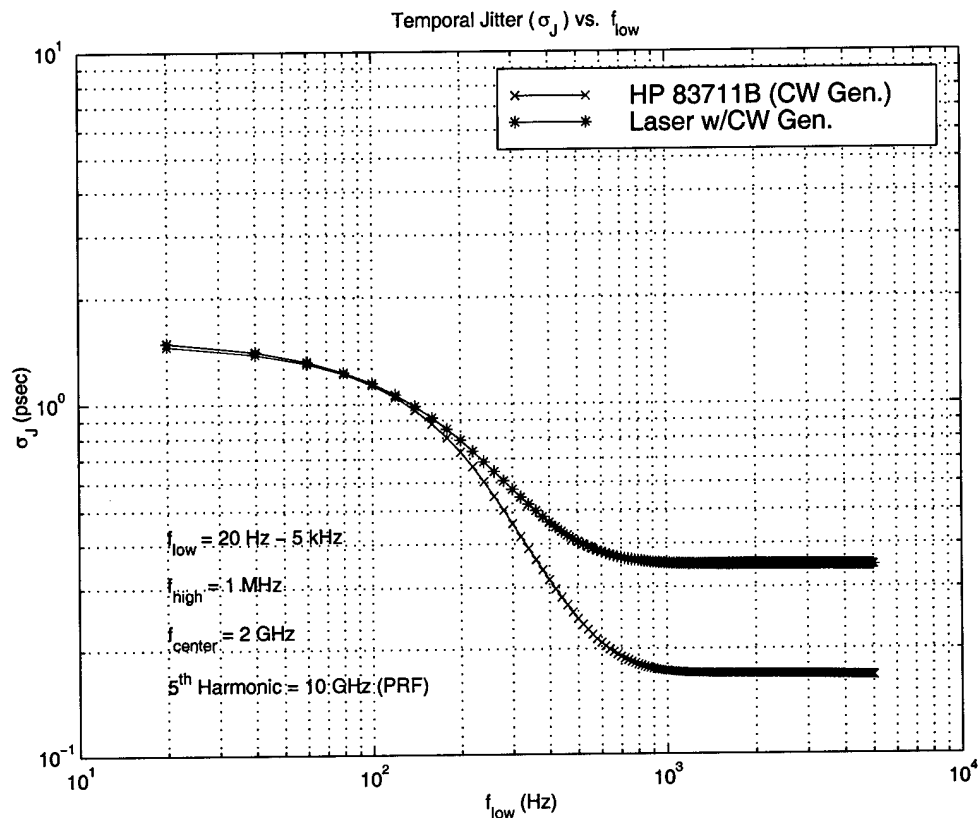


Figure 4.12. CW generator and laser powered by CW generator, timing jitter comparison.

Figure 4.12 shows the results of the temporal jitter comparison for the laser and the cw generator. Numerically, the diagram shows the generator alone with about 1.55 ps of timing jitter and the sigma laser with around 1.65 ps.

A comparison of the sigma laser signal produced with the cw generator and the laser signal produced with the sweep oscillator is also instructive. The importance of this comparison was to solidify the previous assumption that the cw generator was the better microwave signal generator to operate with the sigma laser.

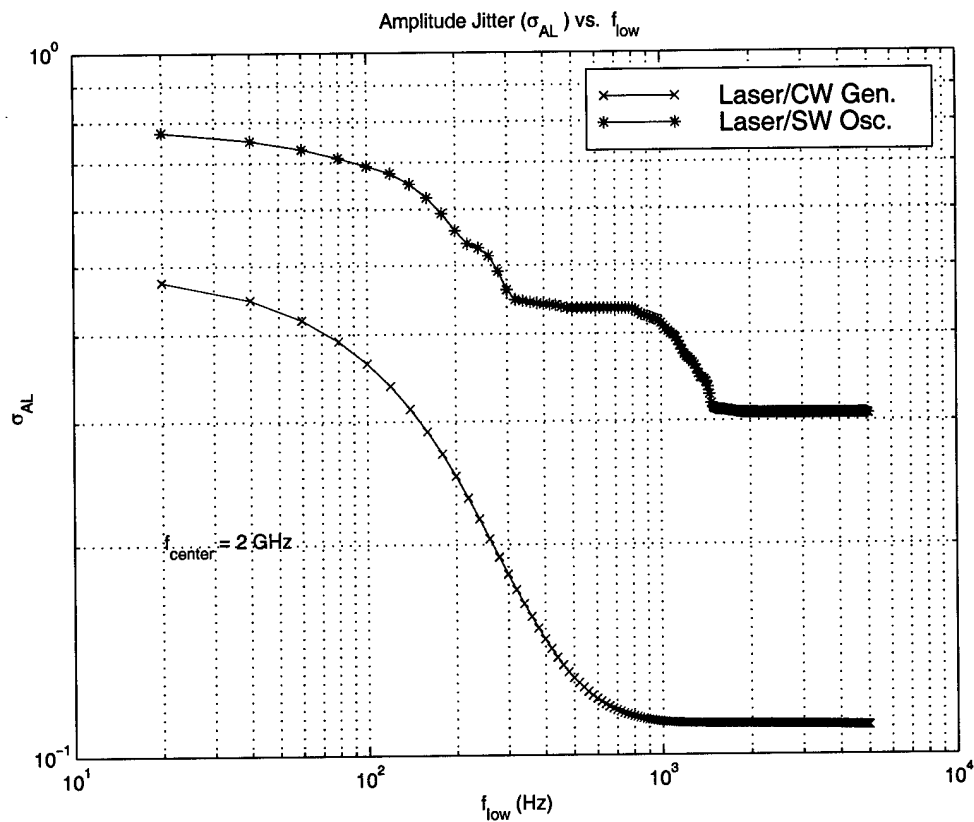


Figure 4.13. Laser powered by CW generator and sweep oscillator, amplitude jitter comparison

Figure 4.13 shows that the amplitude jitter associated with the laser was less when operating with the cw generator as opposed to the sweep oscillator. The maximum amplitude jitter for the laser with the cw generator was measured at $f_{low} = 20$ Hz as 48% while the laser with the sweep oscillator was 78%. There was 30% more jitter or fluctuation in the amplitude of the laser pulse train when powered by the sweep oscillator.

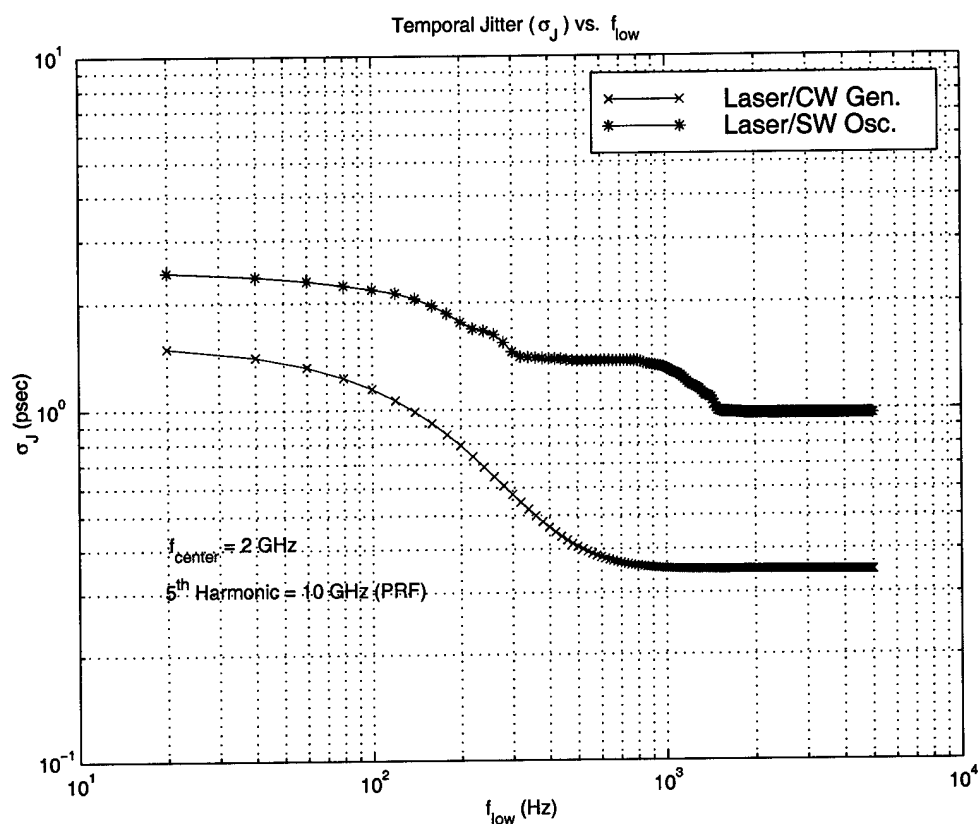


Figure 4.14. Laser powered by CW generator and sweep oscillator, timing jitter comparison.

Figure 4.14 shows the comparison between the temporal jitter of the two laser signals at the 5th harmonic. The graph indicates that there was more timing jitter associated with the laser and sweep oscillator than with the laser and cw generator. Numerically, there was a maximum of 1.65 ps of timing jitter with the laser and cw generator and 2.5 ps with the laser and the sweep oscillator. Not only did the use of the cw generator decrease the total amplitude jitter of the laser, but it also decreased the timing jitter by 0.85 ps.

As previously discussed, the 5th harmonic of the 2 GHz fundamental was used in the preceding temporal jitter measurements with f_{low} initiated at 20 Hz. To garner a more

accurate analysis of the jitter using the developed measurement techniques, the final set of jitter data utilized a 2 GHz fundamental frequency produced by the cw generator. With the use of the cw generator, the ability to resolve the laser signal down to 4 Hz was achieved. Subsequently, the sixth harmonic was also able to be resolved, providing an increase in temporal jitter calculation accuracy.

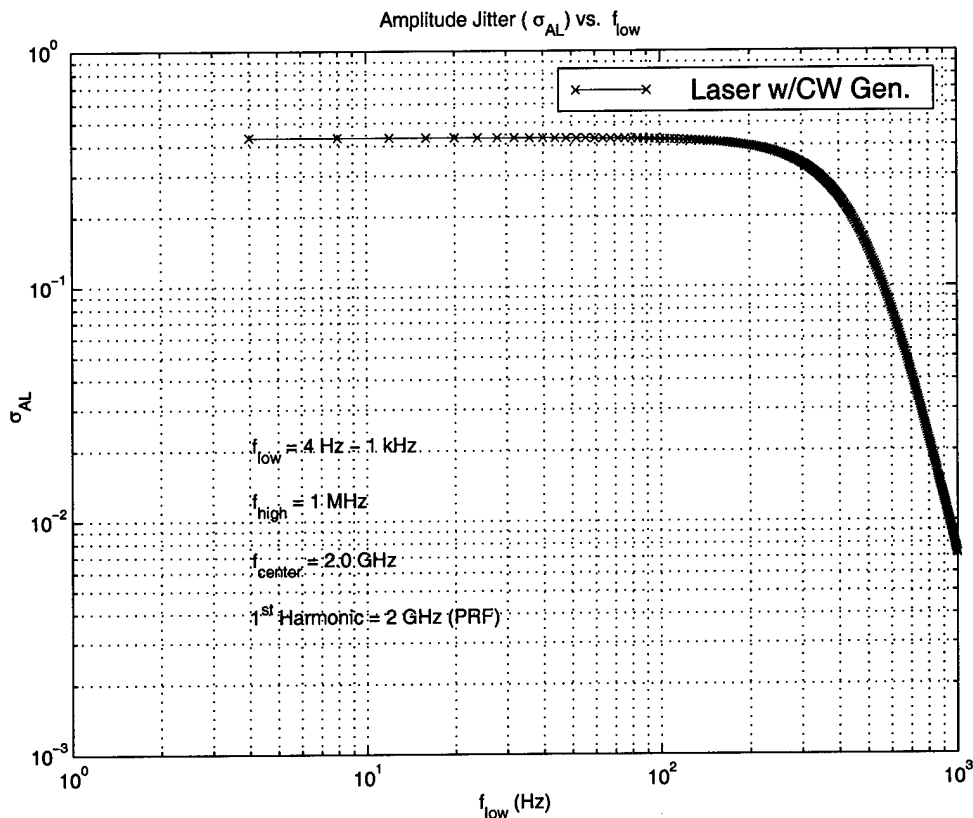


Figure 4.15. Laser powered by CW generator, amplitude jitter at 2 GHz PRF.

Figure 4.15 shows the amplitude jitter for the laser operating with the more stable cw generator at 2 GHz PRF and frequency integration span of 4 Hz to 1 kHz. Although, by accomplishing this sort of resolution, the change in the lower limit of integration span (f_{low}) was reduced from 5 kHz to 1 kHz. Numerically, the maximum amplitude jitter at $f_{low} = 4 \text{ Hz}$ showed little difference from the previous measurement limit of 20 Hz.

In Chapter III it was discussed that the higher the harmonic of a signal, the more accurate the timing jitter calculation would be. For the 2 GHz signal, both the 5th and 6th harmonic were measured. This was accomplished with the goal to compare the timing jitter of both harmonics in order to quantify the effect of the harmonic number (M) in the timing jitter calculation Equation 3.5.

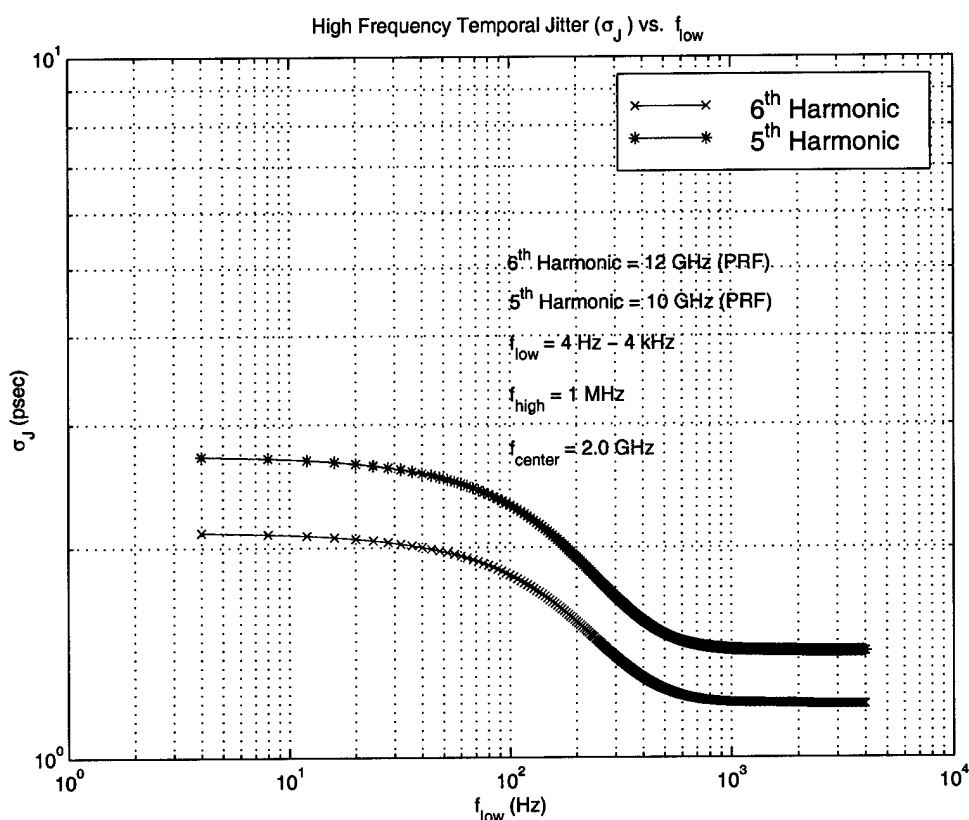


Figure 4.16. Laser powered by CW generator, timing jitter harmonic comparison.

Figure 4.16 shows the comparison of the timing jitter calculation at the 5th and 6th harmonic for the fundamental PRF of 2 GHz. The maximum jitter present at the lower limit of integration of 4 Hz, was 2.1 ps for the 6th harmonic and 2.8 ps for the 5th. This graphic substantiated the premise that timing jitter was directly linked to the harmonic

number. It also showed that at the higher order harmonics the presence of amplitude jitter becomes less.

Tables 4.1 and 4.2 show respectively, the jitter measurement results and the jitter added by the laser cavity, for the sweep oscillator and cw generator. The numerical data was taken from the computer for improved accuracy. The laser cavity data was calculated as the root mean square of the difference between the laser and the signal generators.

$$\sigma_{\text{Laser cavity}} = \sqrt{(\sigma_{\text{Laser+Generator}})^2 - (\sigma_{\text{Generator}})^2} \quad 4.2$$

The different values for the laser cavity in the two tables was attributed to the stability of the signal produced by each respective generator.

	Amplitude Jitter (σ_{AL})	Temporal Jitter (σ_J)
HP 8350B (SW Osc.)	0.56	1.8 ps
Laser w/ SW Osc.	0.78	2.5 ps
Laser cavity	0.54	1.74 ps

Table 4.1. Summary of Jitter Measurements for Laser and Sweep Oscillator at Frequency Span of 20 Hz to 1 MHz. Amplitude Jitter Calculated at Fundamental PRF, Temporal Jitter Calculated at the 5th Harmonic.

	Amplitude Jitter (σ_{AL})	Temporal Jitter (σ_J)
HP 83711B (CW Gen.)	0.46	1.55 ps
Laser w/ CW Gen.	0.48	1.65 ps
Laser cavity	0.14	0.57 ps

Table 4.2. Summary of Jitter Measurements for Laser and CW Generator at Frequency Span of 20 Hz to 1 MHz. Amplitude Jitter Calculated at Fundamental PRF, Temporal Jitter Calculated at the 5th Harmonic.

D. LASER CONTROL AND EFFECTS

The final aspect of this research was the effect of pump laser power and microwave signal generator frequency settings on the stability of the laser pulse train. Two avenues were explored. The first involved a comparison of laser signal strength versus the current produced by the pump laser diode controllers. The second was the effect of amplitude jitter on the laser signal at different fundamental PRFs.

1. Pump Laser Diode Current Setting

The effect of higher and lower current settings for the laser diode controllers driving the optical amplifiers was not known. To analyze this, the laser was connected to the cw generator and run at various current settings ranging from 32 mA of average current to the maximum current allowed for the diodes of 180 mA. Spectrum analyzer data were collected for current settings of 32, 40, 60, 100, 120, 140, 160, and 180 mA. The spectral amplitude was plotted as amplitude in dBm versus frequency. All measurements were taken with the cw generator producing a fundamental frequency of 10 GHz and a spectrum analyzer frequency span of 1 kHz to 500 kHz. Figure 4.17 shows the result of this test. The graph shows that as the current settings are decreased at the laser diode controller starting at 180 mA, the peak amplitude or the strength of the pulse is diminished until the signal strength is at a minimum, at 32 mA. This supported the conclusion that the more current applied to the laser diodes, the stronger the signal produced and possibly the less jitter.

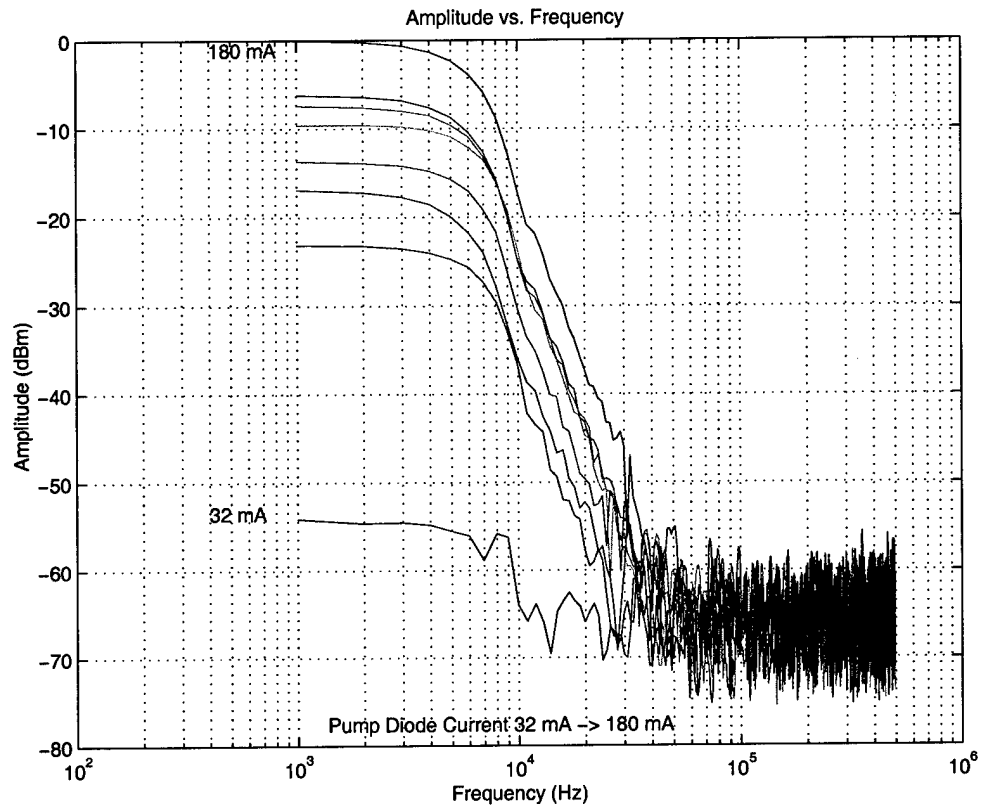


Figure 4.17. Amplitude and frequency of laser signal at various current settings.

2. Signal Generator Frequency Setting

The final analysis consisted of running the laser with the cw generator and comparing the amplitude jitter present at different fundamental frequencies. The laser diode controllers were set to pump 180 mA of current into the laser while data was collected at fundamental frequency settings of 5, 7.5, and 10 GHz. Like the previously discussed laser measurements, the amplitude jitter were measured referenced to f_{low} . The

amplitude jitter was plotted as a ratio. Figures 4.18 shows the results of these measurements.

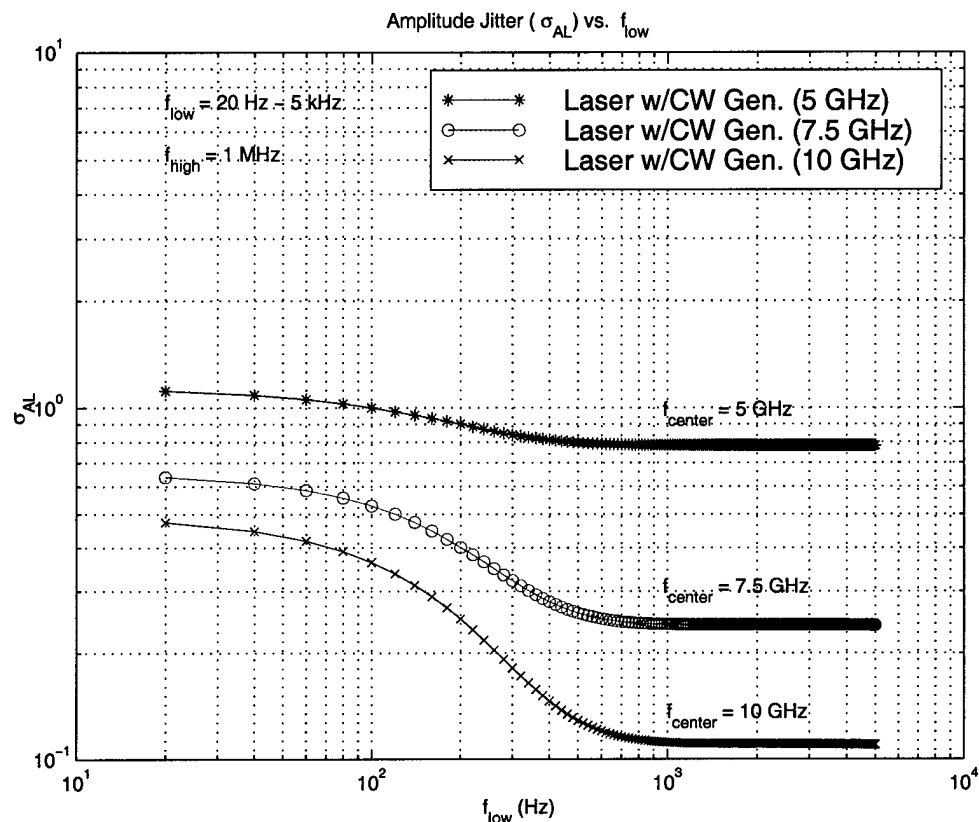


Figure 4.18. Amplitude jitter at various fundamental frequencies.

As can be seen from Figure 4.18, the amplitude jitter decreased as the fundamental frequency programmed into the signal generator increased. Numerically, the value of the maximum jitter present, f_{low} equal to 20 Hz, was calculated from the graph, showing that the amplitude jitter for the 10 GHz signal at approximately 48%, while the 5 GHz was nearly lost in noise.

These tests showed encouraging information for the further development and optimization of the sigma laser for frequency ranges of 10 GHz and higher. If the

amplitude and timing jitter can be minimized at the higher frequencies it will allow the development of an accurate (10 bit), high-frequency (10 GHz) analog-to-digital antenna conversion.

THIS PAGE INTENTIONALLY LEFT BLANK

V. CONCLUSIONS AND RECOMMENDATIONS

A. MEASUREMENT TECHNIQUE

The measurement technique designed in this thesis is useful for the characterization and calculation of amplitude jitter and temporal jitter associated with the sigma mode-locked laser. The programs and procedures written were based on fundamental calculations for the amplitude jitter and higher harmonics (5 and 6 for 2 GHz) for the temporal jitter. It would be beneficial in the future if the available test equipment were suitable to support higher order harmonic analysis for PRFs of 10 GHz and above. This would provide an opportunity to install user-interaction methods for the selecting of specific limits of integration for the jitter calculations. As it stands the limits are set, based on available resolution, in the program itself. A second recommendation would be to install a new RF spectrum analyzer, one that has the ability to resolve discrete data points on the order of 4 to 20 Hz while working with frequency spans in the 1 to 3 MHz regime.

B. LASER DIODES

The laser diodes presently installed in the sigma laser are current limited to 181 mA. These diodes if operated at greater than 210 mA of drive current will have a limited life span. If operated greater than 265 mA, they will be permanently damaged. The thesis research showed the effects of driver current on the final output of the laser signal.

The higher the driver current, the stronger the laser output signal, and the less jitter. To optimize the sigma laser with higher power (higher current limit) diodes would possibly allow for a much more stable output pulse train while minimizing amplitude and timing jitter. This can be achieved with the idea of maintaining the limited size of the laser.

C. DESIGN OF SIGMA LASER

The final recommendation for the sigma laser is in its design. Currently, the laser cavity is sandwiched between two pieces of plexi-glass with four inch spacers. The feedback maintaining loop of the laser would be optimized if the cavity was contained in a plexi-glass box. This would reduce the environmental effects (temperature, atmospherics) that currently plague the laser. By reducing these effects, the reliance on the piezoelectric transducer to maintain cavity length would decrease, thereby reducing any subsequent noise.

D. SUMMARY REMARKS

The goals of this research were varied. They were ultimately tied to the calculation, reduction, and optimization of the laser and its associated jitter. A user-friendly, accurate method of calculating the final output jitter of the laser was designed and implemented. This design utilized a wide bandwidth fast photodetector, a wide bandwidth RF spectrum analyzer, and commercially available computer software. This method was used extensively for the characterization and measurement of the laser

amplitude and timing jitter. This method of analysis will be remarkably helpful in the future as the design of the sigma laser is optimized to reduce overall jitter.

The results of Chapter IV show that the laser pulse train can be optimized by use of the HP83711B Continuous Wave Generator for its microwave signal vice the HP8350B Sweep Oscillator. By using the cw generator, amplitude jitter in the sigma laser was reduced by 10% of the fundamental peak carrier frequency and timing jitter was reduced by .35 ps for the fifth harmonic. Later analysis showed that by measuring the amplitude jitter with the lower limit of the integration span set to 4 Hz provided little difference from the maximum amplitude jitter calculation for the limit of 20 Hz. Also, by measuring the timing jitter in the highest order harmonic available (6th) provided a more accurate value for σ_J . The results also show that above 10 kHz, the upper limit of integration in the noise power equation had no appreciable effect on the final output jitter of the laser. However, the lower limit of integration dramatically reduced the jitter as it was increased. This leads to the conclusion that when jitter is reported by outside sources, the lower limit of integration and for that matter the integration range should always be noted in its entirety. Since the lower limit is directly related to the integration time, ΔT should also be provided.

THIS PAGE INTENTIIONALLY LEFT BLANK

APPENDIX A. MATLAB CODE FOR SOLVING JITTER CALCULATIONS

This appendix shows the programs used for calculating amplitude and timing jitter, and amplitude versus frequency comparisons.

A. AMPLITUDE VERSUS FREQUENCY

The following MATLAB program was used with 8 separate files of data. The program was meant as an aid in comparing the signals from the output of the sigma laser and microwave signal generators.

%File: freqamp_com.m

```
filename1 = 'filename1.txt'
filename2 = 'filename2.txt'
```

```
Fmod = 10e+9; %fundamental frequency set on signal generator
```

```
%*****DATA RETRIEVAL*****%
```

```
fid1 = fopen(filename1);
datahdr1 = fscanf(fid1,'%76c',7); %skip first 7 lines of data file (header/date info)
format long e
a1 = fscanf(fid1,'%g %g',[2,1000]); %establish matrix with 2-rows, 1000-columns
freq1 = a1(1,:);
amp1 = a1(2,:);
status1 = fclose(fid1); %close file once data is extracted
```

```
z1 = [];
z1 = amp1/10;
Pmw1 = 10.^z1; %convert amplitude from dBm to mW
Freq_hz1 = freq1;
Amp_db1 = amp1;
```

```
table1 = [freq1, Pmw1]; %place values for frequency and power in matrix
[i1,j1] = max(table1(:,2)); %find the maximum power cell in data matrix
Fc1 = table1(j1,1); %find value of peak frequency corresponding to
Maximum power
```

```
%Above process is repeated for filename2.
```

```
.
.
.
```

```
%****FIND DATA IN TABLE BETWEEN PEAK FREQUENCY AND 500 kHz****%
```

```

data_table1 = [freq_hz1,amp_db1];
data_table2 = [freq_hz2,amp_db2];

[k,l] = max(data_table1(:,2));      %find max amplitude from table
[m,n] = max(data_table2(:,2));

dBmax1 = data_table1(l,2);          %assignment of max amplitude
dBmax2 = data_table2(n,2);

Fc11 = (Fc1);
Fc12 = (Fc1 + 500000);              %setting limits of table search
Fc21 = (Fc2);
Fc22 = (Fc2 + 500000);

%find data in tables between reference frequencies
Points1 = find(data_table1(:,1)>Fc11 & data_table1(:,1)<Fc12);
Points2 = find(data_table2(:,1)>Fc21 & data_table2(:,1)<Fc22);

Val1x1 = data_table1(Points1,1);    %assign variable the frequency data points found
Val2x1 = data_table2(Points2,1);    %between set limits

A = [Val1x1];                       %place data in matrix
Val1xx1 = (A-Fc1);                  %subtract peak frequency from value to get span
B = [Val2x1];
Val2xx1 = (B-Fc2);

Val1y1 = data_table1(points1,2);    %assign variable the amplitude data points found
Val1y2 = Val1y1 - dBmax1;           %subtract max amplitude to reference points to dBc
Val2y1 = data_table2(points2,2);
Val2y2 = Val2y1 - dBmax2;

figure(1)
semilogx(Val1xx1, Val1y2, '-xr',Val2xx1, Val2y2, '-*b')
xlabel('units')
ylabel('units')
legend('1st device', '2nd device')

```

Program A1: MATLAB program used to compare the amplitude versus frequency for up to 8 files of data.

B. AMPLITUDE AND TIMING JITTER

The following MATLAB program was used to import data files stored in '.txt' format and solve for the amplitude and timing jitter. Each piece of equipment tested had two files of data taken. The first was for a frequency span of 20 kHz, the second for a span of 2 Mhz. The form of the program as it stands was used to combine the two files of data and calculate the jitter as the lower limit of integration (Δf_{low}) was changed from 20 Hz to 5 kHz. The graphs produced by this program were covered in Chapter IV.

%File: jitter.m

```
filename1 = 'filename1.txt'      %filename of 20 kHz data
filename2 = 'filename2.txt'      %filename of 2 MHz data

Fmod = 10e+9;                   %fundamental frequency set on signal generator

span1 = 20000;                  %frequency span (20 kHz) set on spectrum analyzer
span2 = 2000000;                %frequency span (2 MHz) set on spectrum analyzer

rbw1 = 300;                     %resolution bandwidth set on spectrum analyzer
rbw2 = 10000;                   %rbw2 = 10 kHz

%*****DATA RETRIEVAL AND JITTER CALULATIONS*****%
%FILE ONE (20 kHz)
fid1 = fopen(filename1);
datahdr1 = fscanf(fid1,'%76c',7); %skip first 7 lines of data file (header/title)
format long e
    a1 = fscanf(fid1,'%g %g',[2,1000]);
    freq1 = a1(1,:);              %similar to program A1
    amp1 = a1(2,:);
    status1 = fclose(fid1);

z1 = [];
z1 = amp1/10;
Pmw1 = 10.^z1;                  %convert amplitude from dBm to mW
freq_hz1 = freq1;
amp_db1 = amp1;

table1 = [freq_hz1, Pmw1];      %place frequency and power data in matrix
[i1,j1] = max(table1(:,2));     %find max value of mW
Pmw_max1 = max(Pmw1);
Fc1 = table1(j1,1);            %find corresponding peak frequency
delta_f1 = span1./1000;         %distance between data points ( $\Delta f$ ) for file 1
T1 = 1./Fmod;                  %pulse repetition interval
```



```

fh1 = 10000; %fhigh for first integral
y1 = Fc1 + fh1; %upper limit of integration for 1st integral
jj1 = 0;
Pf_Sum1 = [];

for fl1 = 20:20:5000 %loop for changing flow from 20 Hz to 5 kHz in
                    steps of 20 Hz

    clear value
    jj1 = jj1+1; %counter
    x1 = Fc1 + fl1; %lower limit of integration for 1st integral

    %Find all data in table between the upper and lower limits of integration.
    data1 = find(table1(:,1)>x1 & table1(:,1)<y1);
    value1 = table1(data1,2); %amplitude values corresponding to frequency
                              values between limits of integration.
    Pf_Sum1(jj1) = sum(value1); %summation of all frequency values between
                                limits of integration.
    plotFL1(jj1) = fl1 %all of the Δflow values

end

%Jitter calculations
m = harmonic number
Noise_Power1 = ((2/rbw1)*delta_f1).*Pf_Sum1; %noise power of signal
SigmaAL1 = sqrt(Noise_Power1/Pmw_max1); %amplitude jitter
SigmaJHF1 = (1/(2*pi*Fc1*m))*SigmaAL1; %timing jitter

SigmaAL_data1 = SigmaAL1'; %transpose of row vector
SigmaJHF_data1 = SigmaJHF1';

%*****%
%FILE TWO (2 MHz)
fid2 = fopen(filename2);
datahdr2 = fscanf(fid2,'%76c',7);
format long e
a2 = fscanf(fid2,'%g %g',[2,1000]);
freq2 = a2(1,:);
amp2 = a2(2,:);
status2 = fclose(fid2);

z2 = [];
z2 = amp2/10;
Pmw2 = 10.^z2; %convert amplitude from dBm to mW
freq_hz2 = freq2;
amp_db2 = amp2;

```

```

table2 = [freq_hz2,Pmw2];
[i2,j2] = max(table2(:,2));           %find max value of peak power
Pmw_max2 = max(Pmw2);
Fc2 = table2(j2,1);                   %find corresponding center frequency
delta_f2 = span2./1000;               %distance between data points ( $\Delta f$ ) for file 2
T2 = 1./Fmod;                         %pulse repetition interval

fl2 = 10000;
x2 = Fc2 + fl2;                       %flow for second integral (fpeak+10 kHz)
fh2 = 1000000;
y2 = Fc2 + fh2;                       %fhigh for second integral (fpeak+ 1 MHz)

data2 = find(table2(:,1)>x2 & table2(:,1)<y2); %data retrieval between limits
value2 = table2(data2,2);
Pf_Sum2 = sum(value2);                %sum data between limits

%Jitter calculations
Noise_Power2 = ((2/rbw2)*delta_f2).*Pf_Sum2; %PN for file two
SigmaAL2 = sqrt(Noise_Power2/Pmw_max2);      % $\sigma_{AL}$  for file two
SigmaJHF2 = (1/(2*pi*Fc2*m))*sigmaAL2;       % $\sigma_{JHF}$  for file two

SigmaAL_data2 = SigmaAL2';
SigmaJHF_data2 = SigmaJHF2';

%Total Jitter for two files
sigmaAL_total12 = (SigmaAL1 + SigmaAL2)';
sigmaJHF_total12 = (SigmaJHF1 + SigmaJHF2)';

sigmaJHF_total12p = (sigmaJHF_total12 * 1e+12); %convert to picoseconds
.
.
.
%Continue for 3 more sets of files (20 kHz, 2 MHz)
.
.
.
%graphic analysis and comparisons can now be done using (flow = plotFL#),  $\sigma_{AL}$ ,  $\sigma_{JHF}$ 

```

Program A2: MATLAB program used to calculate and graph amplitude and timing jitter for 4 sets of data files.

THIS PAGE INTENTIONALLY LEFT BLANK

APPENDIX B. OPERATION OF THE SIGMA LASER

A. SIGMA LASER OPERATION

There are four basic steps to operation of the sigma laser. In order, they include the pump diode temperature control, pump diode current control, modulation, and setup of the autocorrelator or photo-detector. The laser output pigtails should be connected to the autocorrelator or photo-detector and the feedback detector. The longest pigtail should be connected to the autocorrelator through an ST/ST fiber connector. A second cable connects the laser output to the autocorrelator using a FC connector. If the cover of the autocorrelator is to be removed during laser operation, or the laser output pigtail is moved to another device, then the Kentek "Near IR and CO₂" # SES-BW laser safety spectacles must be worn for safety purposes. **Warning**, the sigma laser is a pulsed laser with invisible output at 1560nm. It can cause eye damage. If the photo-detector is being used, the pigtail should be connected to the input of the photo-detector using a ST single-mode connector, with a SMA-RF connector on the output of the photo-detector.

1. Pump Diode Temperature Controller Operation

Warning, without proper cooling, the laser diodes will overheat and fail permanently. The green light indicating temperature controller output is in a position where it is difficult to see. This light should be triple checked before turning the SDL 800 laser diode controller pump current on.

- Front settings for the temperature controllers are as follows:

<u>Switch/Button/Knob</u>	<u>Setting</u>
Power	ON
Limit	1.5
Set R	10.00 K Ω using large control knob.

After turning the power on, if the “Open Therm” remains on, double-check the cable connections. If it still remains on, turn the unit off and seek assistance.

- Switch the “Display Mode” from “Set R” to “Actual R” and read the resistance on the LED display.
- Press “Output” to start cooling the laser diodes. The LED should change to 10.00 K Ω . The green output light under the large knob should come on.
- Verify that the “Display Mode” is set to “Actual R,” the LED display reads 10.00 K Ω , and the output light is on.

The temperature controllers tend to drift during operation and may be adjusted back To 10.00 k Ω while in operation. During the start of cooling, the “Limit” indicator may flash briefly; however, if it stays on, turn the output off and seek assistance.

2. Pump Diode Laser Controller Operation

Warning, turning on the laser output with “Average Current” other than zero will probably ruin the laser diode. The highlighted LED’s next to the selection options are easily misread as to which option is selected. Furthermore, the selection buttons are sticky and may click down to another selection inadvertently. The “laser on” button often sticks and the device will let the user turn the current up to the desired level while

in setup mode without any other warning. If this occurs, turn the current down and then turn the laser on. The user should double check that the highlighted LED is next to “Average Current” and that 0 mA is set prior to pumping current through the laser diode.

- The SDL 800 laser controller operational settings are as follows:

<u>Switch/Button/Knob</u>	<u>Setting</u>
Power	On using key switch.
Current Limit	191 mA using current limit knob.
Average Current	0 mA using bias level knob.
Setpoint Temp.	unused
Det. Cal.	Unused

- Verify that the laser diode controller “Average Current” is 0 mA.

Warning, laser light not contained in fiber or equipment can be an eye hazard.

- Verify that the laser output pigtails are connected to the autocorrelator or photo-detector, and the feedback detector.
- Push the button next to “Laser” to switch from “Setup” to “On”.

The setup LED will flash for approximately 5 seconds and then the device will turn the laser diodes on. If the controller turns on the “Error” light instead of the “On” light, turn the controller off by the key, double check all cable connections and try again. If the “Error” light comes on again, turn the controller off and seek assistance.

- Verify that the temperature controller green “Output” lights are lit and the “Actual R” on both controllers is 10.00 k Ω .

- Verify that the control option is set to “Average Current”, if not, select this option using the buttons outside of the indicating arrows, the appropriate LED will be lighted.
- Slowly turn the “Bias Level” knob until the display reads 15 mA of “Average Current”. Then turn the current up until 180 mA is attained.

At 180 mA, each diode pumps 100 mW of 980 nm laser light into the erbium-doped fiber in the laser. **Warning**, operating the laser diodes at greater than 210 mA of drive current will shorten the life of the diode. Operating the diode greater than 265 mA will damage the diode permanently [Ref. 8]. The error light will flash if drive current is within 10 mA of the current limit [Ref. 9]. If this occurs, double check that the current limit is set at 191 mA. If the error light comes on while turning the current up, seek assistance. This is a sign that the laser diode has failed. The resistance displayed on the temperature controllers will drop slightly by a few tenths of a $k\Omega$ while turning the current up on the diodes. If the resistance does not return to the set point within a few seconds or the resistance continues to drop, turn the laser controller current down to zero and seek assistance.

3. Modulation

a. DC Bias Voltage

A modulator bias voltage of +14.45 Vdc works well for normal operation. Different bias voltages can be used based on experimentation. If attempting to harmonically mode-lock the laser to attain a PRF of twice the modulation, then +15.9

Vdc should be used as a starting point. A digital multimeter should be used to monitor the DC power supply voltage.

Warning, a bias voltage of higher than 20 Vdc may run the E-TEK modulator; do not exceed this voltage or the sigma laser will remain inoperable until a new modulator is spliced into the laser cavity.

- Turn on the Model 5005S DC power supply and the attached digital multimeter.
Verify +14.45 Vdc.

b. Signal Generator

Ideally, the HP83711B CW Generator should be turned on without transmitting a signal for a few hours prior to operation. A modulation frequency of 10.1 GHz is a good starting point but values between 5.1 and 12.1 GHz have successfully been used.

- HP83711B CW Generator settings are as follows:

<u>Switch/Button/Knob</u>	<u>Setting</u>
Power	ON
Frequency	depress "FREQ"
Keypad	type in "10.1 GHz"
Power	depress "POWER LEVEL"
Keypad	type in "15.2 dBm"
ALC Mode	INT

The "unleveled" light should be extinguished at this point. If not, try turning the generator off and then on. The signal generator is power limited at higher frequencies.

This means that the “unleveled” light can also be extinguished by reducing the power level. If this does not work, seek assistance from the microwave lab.

c. MITEQ Microwave Amplifier Operation

- Turn on the MITEQ amplifier by turning on the Model 3650S power supply. Ensure that it is set for +15 Vdc.

4. Autocorrelator Operation

The laser is mode-locked while watching for pulse formation on the oscilloscope next to the autocorrelator. The laboratory overhead lights directly above the autocorrelator must be turned off because they interfere with the highly sensitive photomultiplier tube inside the device even with the lid on.

- The attached oscilloscope settings are:

<u>Switch/Button/Knob</u>	<u>Setting</u>
Power	ON
CH1 V/Div	0.1 V (initially)
Sec/Div	2 ms (initially)

- Turn the autocorrelator on using the unmarked switch on the front; the green light directly above it will come on.
- Rotate the laser output polarization controller (PC) on top of the laser until a pedestal of noise appears on the left side of the scope. Maximize the pedestal using the PC.

The FC connector cable attached to the autocorrelator occasionally interferes with the polarization control. If the PC appears ineffective, carefully rotate the yellow output cable until the maximum pedestal of noise appears. Further maximize the pedestal using the PC.

- Change the oscilloscope Sec/Div to 1ms.

The autocorrelator is connected directly to the computer using a standard computer connection cord plugged into the back of the autocorrelator. This should be accomplished prior to any work on the laser. Measurements can then be made on the signal using the installed autocorrelator software.

5. Photodetector and Spectrum Analyzer Operation

If the autocorrelator is not used then the alternative option is to use the NEWPORT D-15ir Detector coupled with the HP8566B Spectrum Analyzer.

- Turn on the NEWPORT detector using the black switch on top. The red "ON" light should be lighted. If the red "LOW" light is lit then secure the laser, and replace the AAA battery in the photo-detector.
- The attached Spectrum Analyzer setting are as follows:

<u>Switch/Button/Knob</u>	<u>Setting</u>
Power	ON
Frequency	Depress "CENTER FREQUENCY"

Keypad	Type in the frequency the CW Gen. is set to
Span	Depress "FREQUENCY SPAN"
Keypad	Type in 2.0 MHz (initially)
Bandwidth	Depress "RES BW", adjust to 3 kHz

The frequency span is directly related to the resolution bandwidth. For higher frequency spans, higher resolution bandwidth is needed. For example a frequency span of 20 kHz only requires a resolution bandwidth of 300 Hz. The spectrum analyzer is directly coupled to the computer using a standard computer connector cable plugged into the J7 port on the back of the analyzer. Spectrum data can then be retrieved using the installed software on the computer.

For procedure and pre-operational set up of the integrating amplifier, feedback maintaining loop, and mode-locking technique refer to Ref. 2, pages 137-140.

6. Autocorrelator Software

The laser pulsewidth can be measured using an oscilloscope. This measurement is in milliseconds and a series of calculations must be made using the formulas in the operator's manual. The best analysis is accomplished by using the Femtochrome software on the computer.

- Double click on the MS-DOS icon or open MS-DOS window from the Windows 95 start menu. The program executable is "C:\Femto\FR_CDA". Alternatively, there are batch (bat) files in the default MS-DOS "C:\Windows" and the "C:\Femto" directories.
- Type the word "femto" and the program will start.

- During program initialization, type "2" for COM2 and type "0" for rapid scan.
- When instructed, press the reset button on the back of the autocorrelator next to the wall power connection.
- The delay knob on the autocorrelator is useful for centering the pulse on the computer screen.
- Press the black button next to the delay knob and turn the delay knob so the pulse is centered about the third time division from the left on the oscilloscope screen. This will nearly center the pulse on the computer. The delay can be further adjusted as necessary.

The software program is not set up to print directly to printer due to a mismatch in MS-DOS programming and the advanced printers used in the lab. The program will print the plot to a graphics file or will print the numerical data to a text file.

7. Spectrum Analyzer Software

When using the photo-detector with the spectrum analyzer, the best way to capture data is by using the LABVIEW 4 software on the computer. The software by itself will not do calculations or measurements, but it will allow the user to capture the laser signal being generated on the spectrum analyzer in 1000 data points.

- With a signal centered on the spectrum analyzer, double click on the "Moose.llb" icon, located on the Windows 95 screen.
- A "File Dialog" box will appear. Highlight "Moose.vi" and click "OK".

- A graphical screen will appear. To capture the image that is on the spectrum analyzer, click on the white “right arrow” located in the upper left hand corner of the screen.
- The image located on the spectrum analyzer will appear on the graphical display with the numerical values of the 1000 data points located above it. The graph uses frequency (Hz) for the x-axis, and amplitude (dBm) for the y-axis.
- To save an image, click on the “save to file” icon on the graphics screen. It should turn yellow indicating that the program is ready to save the next captured image.
- Enter the path and file name of the data to be saved. Be sure to add “.txt” to the end of the file name. This will save the file as a text file for later use in MATLAB.
- Once the filename and path are entered and the icon is yellow, click on the “right arrow” again. This will capture the image on the spectrum analyzer and save it to a file.
- Click the “save to file” icon again to turn it white. If this is not done, then the next time that the “right arrow” is clicked on, then the data for the new image will be subtended onto the end of the last file saved.

This software is useful for capturing the data used in MATLAB for measuring the jitter of the signal.

8. Turning Off the Sigma Laser

The order for securing the sigma laser is important. Most importantly the temperature controllers must remain on until the drive current through the diodes is reduced to zero.

- Turn off the bias voltage and the +15 Vdc power supplies.
- Turn off the signal generator.
- Turn the "Average Current" using the "Bias Level" knob on both laser diode controllers down to zero. "Current Limit" should still be 191 mA.
- Switch the laser diode controllers from "ON" to "Setup".
- Turn off the laser diode controllers using the keys.
- Turn off the Autocorrelator or the photo-detector.
- Turn off the output to the temperature controllers; the resistance should change. If the resistance drops significantly to 9 k Ω or less, turn the output back on and let the diodes cool for a while.
- Turn the temperature controllers, oscilloscopes, multimeters, and spectrum analyzer off.
- Turn the feedback detector off using the button on top. **Warning**, the microwave amplifiers nearby will be hot. Check that the "Power On" light is extinguished. If the detector is left on, the batteries will need to be replaced the next time the laser is to be operated.

THIS PAGE INTENTIONALLY LEFT BLANK

LIST OF REFERENCES

- [1] Henry F. Taylor, "An Optical Analog to Digital Converter – Design and Analysis," *IEEE Journal of Quantum Electronics*, vol. 15, no. 4, pp. 210-216, 1979.
- [2] Phillip E. Pace, "Advanced Techniques for Digital Receivers," Technical Report, Naval Postgraduate School, Monterey, CA, 2000.
- [3] Phillip E. Pace and John P. Powers, "Photonic Sampling of RF and Microwave Signals," *Technical Report*, Naval Postgraduate School, Monterey, CA, 1998.
- [4] James M. Butler, "Construction and Measurement of an Actively Mode-Locked Sigma Laser," *Master's Thesis*, Naval Postgraduate School, Monterey, CA, 1998.
- [5] Lasertron, *1996/97 Product Guide*, Burlington, MA, pp. 29-71, 1996.
- [6] Newport Corp., *Photodetector Model D-15ir-ST Users Manual*, Irvine, CA, pp. 8, 1996.
- [7] D. von der Linde, "Characterization of the Noise in Continuously Operating Mode-Locked Lasers," *Applied Physics B*, vol. 39, pp. 201-217, 1986.
- [8] Ursula Keller, Kathryn D. Li, Mark Rodwell, and David M. Bloom, "Noise Characterization of Femtosecond Fiber Raman Soliton Lasers," *IEEE Journal of Quantum Electronics*, vol. 25, no. 3, pp. 280-288, 1989.
- [9] Ross L. Finney and George B. Thomas Jr., *Calculus*, 2nd edition, Addison-Wesley Publishing Co, Reading, MA, pp. 282, 1994.
- [10] Spectra Diode Labs, *SDL 800 Laser Diode Driver User's Manual*, San Jose, CA, 1986.
- [11] Hewlett Packard Co., *HP8350B Sweep Oscillator*, Palo Alto, CA, 1983.
- [12] Thomas F. Carruthers and I. N. Dulling III, "A High-Repetition Rate Ultrafast Fiber laser for Fiber-Optic Communications Systems," *Technical Report*, Naval Research Laboratory, Washington D.C., 1996.
- [13] Eva Part-Enander and Anders Sjoberg, *The Matlab 5 Handbook*, Addison-Wesley Publishing Co, Harlow, England, 1999.
- [14] The MathWorks Inc., *MATLAB Reference Guide*, Natick, MA., 1992.
- [15] The MathWorks Inc., *MATLAB Users Guide*, Natick, MA., 1993.

- [16] Colin R. Cooper, "Introduction to Matlab," EC1010 Course Notes, Naval Postgraduate School, Monterey, CA, 1996.
- [17] J. B. Schlager, Y. Yamabayashi, D. L. Franzen, and R. I. Juneau, "Mode-Locked, Long-Cavity, Erbium Fiber Lasers with Subsequent Soliton-Like Compression," *IEEE Photonics Technology Letters*, vol. 1, no. 9, pp. 264-266, 1989.
- [18] D. J. Derrickson, A. Mar, and J. E. Bowers, "Residual and Absolute Timing Jitter in Actively Mode-Locked Semiconductor Lasers," *IEEE Electronics Letters*, vol. 26, no. 24, pp. 2026-2028, 1990.
- [19] M. E. Fermann, M. Hofer, F. Haberl, and S. P. Craig-Ryan, "Femtosecond Fibre Laser," *IEEE Electronics Letters*, vol. 26, no. 20, pp. 1737-1738, 1990.
- [20] Arthur James Lowery, Noriaki Onodera, and Rodney S. Tucker, "Stability and Spectral Behavior of Grating-Controlled Actively Mode-Locked Lasers," *IEEE Journal of Quantum Electronics*, vol. 27, no. 11, pp. 2422-2430, 1991.
- [21] A. Finch, D. Burns, X. N. Zhu, W. E. Sleat, and W. Sibbett, "Noise Characterisation of Mode-Locked Laser Sources using High-Speed InGaAs Photodetectors," *IEEE Applications of Ultrashort Pulses for Optoelectronics Colloquium*, London, UK, 1989.
- [22] M. J. W. Rodwell, D. M. Bloom, and K. J. Weingarten, "Subpicosecond Laser Timing Stabilization," *IEEE Journal of Quantum Electronics*, vol. 25, no. 4, pp. 817-827, 1989.
- [23] P. E. Pace, S. A. Bewley, and J. P. Powers, "Fiber Lattice Accumulator Design Considerations for Optical $\Sigma\Delta$ Digital Antennas," *Technical Report*, Naval Postgraduate School, Monterey, CA, 1998.
- [24] J. M. Butler, P. E. Pace, and J. P. Powers, "Experimental Results of a Low-Power Sigma Mode-Locked Fiber Laser for Applications in Mobile Sampling of Wideband Antenna Signals," *Technical Report*, Naval Postgraduate School, Monterey, CA, 1998.

INITIAL DISTRIBUTION LIST

1. Defense Technical Information Center 2
8725 John J. Kingman Rd., STE 0944
Ft. Belvoir, VA 22060-6218

2. Dudley Knox Library, Code 52 2
Naval Postgraduate School
411 Dyer Rd.
Monterey, CA 93943-5002

3. Chairman, Code EC 1
Department of Electrical and Computer Engineering
Naval Postgraduate School
Monterey, CA 93943-5121

4. Chairman, Code PH 2
Department of Physics
Naval Postgraduate School
Monterey, CA 93943-5121

5. Associate Professor Phillip E. Pace, Code EC/Pc 1
Department of Electrical and Computer Engineering
Naval Postgraduate School
Monterey, CA 93943-5121

6. Professor James H. Luscombe, Code PH 1
Department of Physics
Naval Postgraduate School
Monterey, CA 93943-5121

7. Professor John P. Powers, Code EC/Po 1
Department of Electrical and Computer Engineering
Naval Postgraduate School
Monterey, CA 93943-5121

8. Commanding Officer 1
Naval Research Laboratory
(Attn: Dr. Irl Duling III, Code 5670)
Optical Sciences Division
4555 Overlook Ave, SW
Washington D.C. 203075

9. Commanding Officer..... 1
Naval Research Laboratory
(Attn: Dr. Tom Carruthers, Code 5670)
Optical Sciences Division
4555 Overlook Ave, SW
Washington D.C. 203075
10. Commanding Officer..... 1
Naval Research Laboratory
(Attn: Dr. Mike Dennis, Code 5670)
Optical Sciences Division
4555 Overlook Ave, SW
Washington D.C. 203075
12. Director, NPS Center for Reconnaissance Research, Code EC/Po..... 3
Naval Postgraduate School
Monterey, CA 93943-5121
11. LT James A. Anderson..... 2
406 Warley St.
Portsmouth, RI 02871